Waveguide Arc Restrike Test Results

Tom Powers, Doug Curry, Kirk Davis, Larry King, and Mike Tiefenbach
Thomas Jefferson National Accelerator Facility
(Test dates July 6, 2004 through September 2, 2004)
JLAB-TN-04-0039

Abstract

The following presents the test setups and results for a series of experiments done on cavity SL16-5 in the CEBAF accelerator. The initial purpose of the experiments was to determine the minimum time that is required before open loop gradient can be reestablished in a cavity after an arc trip. Once it was determined that gradient could be reestablished within 10 ms, a second experiment was performed to determine if stable gradient could be reestablished after a cavity arc trip. This second experiment made use of a connectorized closed loop gradient control system. While the data indicated that one can reestablish gradient within 30 ms after a waveguide vacuum arc, instabilities were observed in the cavity gradient signal which were determined to be microphonic in nature. These microphonic effects were quantified using a cavity resonance monitor and a Voltage Controlled Oscillator- Phase Locked Loop RF system (VCO-PLL). Adding the RF power required to maintain the stable cavity gradient to the RF power required for beam loading may limit the ability to reestablish beam current in the cavity. Further the experimental results indicated that recovery of stable cavity gradient after an electronic quench may not be possible for at least a few hundred milliseconds after the event.

Background

Definition of "Recovery"
There are two arc recovery conditions relating to a superconducting cavity. The first is to apply RF to the cavity and establish a stable gradient. The second condition is to reestablish beam current in the cavity. The first typically has a klystron power margin of several kilowatts while the second typically has a klystron power margin of a few hundred watts.

Cavity Waveguide Configuration
Standard CEBAF cavity structure has two vacuum spaces. The first is the Waveguide vacuum space. It lies between the warm window, which may be ceramic or polyethylene, and a cold ceramic window. The waveguide vacuum space is instrumented with an ion pump and power supply, that has a response time of approximately 15 ms. This ion pump is separated from the waveguide by a tube approximately 40 cm long and 40 mm in diameter. Additionally, the waveguide vacuum is pumped by the cold waveguide and window surfaces. The waveguide temperature transitions from room temperature to 2 K. The cold window is maintained at 2 K when the cryomodule is cold. Calculations indicate that the recovery of the vacuum within the waveguide should be much faster than the 250 ms indicated by the ion pump power supply. [1] The second vacuum space is the cavity vacuum space which is instrumented with a beam line ion pump which, for the cavity under test, is several meters of cold surface away from the cold window.

Types of Arcs

The arcing phenomena in CEBAF cavities was studied extensively in the early nineties. Several papers and technical notes were written on the topic most of which were also published at workshops and conferences. [2, 3, 4, 5, 6, 7] During those studies two types of arcing phenomena were documented. The first type is called a waveguide vacuum arc. This type of event occurs only in the vacuum space between the warm and cold windows. It is characterized by a decay in the cavity gradient that is limited by the external Q of the cavity and impedance of the combination of the discharge and the waveguide load. Typical decay times are 1 ms to 2 ms.

The second type of event is called an electronic quench. This type of event occurs in the vacuum space on the cavity side of the cold window. When this type of event occurs the cavity gradient decays in times between 100 ns and a few hundred microseconds. Electronic quenches are accompanied by large amplitude, short duration X-ray pulses of approximately 500 kRad/hr for less than 5 μs and a quick intense light pulse, a few microseconds in duration, which is detected at the beam pipe and on both the cavity and waveguide side of the ceramic window. The theory is that a burst of gas is injected into the accelerating field of the cavity. The electrons are stripped off and accelerated by the gradient until they strike the beam pipe and release a large dose of X-rays. The energy stored in the cavity (5 to 25 Joules) accelerates these electrons.

When either type of arc occurs in a closed loop RF control system, the control system responds to a reduction in cavity gradient by increasing the forward power significantly. In the case of an electronic quench this rapid increase in forward power will frequently lead to a waveguide vacuum arc. The arc detector electronics has a time delay of 512 μs. If an electronic quench occurs that is not accompanied by a forward power driven waveguide arc, it will be recorded in the control system as a quench fault. The only way it will be detected as an arc fault is if it is accompanied by a forward power driven waveguide arc. Thus the only way to determine which type of event initiated an arc is to analyze the transmitted power signal and determine the fall time. Fall times on the order of one millisecond indicate a waveguide vacuum arc. Fall times much less than 1 ms indicate an electronic quench.

RF Power Requirements for Cavity Operation

The forward power required of a "tuned" cavity in the absence of beam current is given by:

$$P_{Klystron} = \frac{1}{Q_L} * \frac{(\beta + 1)}{4\beta} * E^2 * \frac{L}{(r/Q)} \qquad (1)$$

Adding in-phase beam current increases the required power to the following.

$$P_{Klystron} = \frac{1}{Q_L} * \frac{(\beta + 1)}{4\beta} * (E + IQ_L(r/Q))^2 * \frac{L}{(r/Q)} \qquad (2)$$

If the cavity is detuned, the beam current is not in phase with the cavity RF-fields and the amount of detuning, δf , is much less than the cavity resonant frequency, f_0, additional terms are added to equation (2) and it takes the form of equation (3): [8]

$$P_{Klystron} = \frac{L}{R_C} * \frac{(\beta+1)}{4\beta} * \left\{ \left(E + I_0 R_C \cos\psi_B\right)^2 + \left(2Q_L \frac{\delta f}{f_0} E + I_0 R_C \sin\psi_B \right)^2 \right\} \quad (3)$$

Where:

$$R_C = Q_L (r/Q) \quad (4)$$

β is the RF coupling factor given by:

$$\beta_{Overcoupled} = \frac{1+\frac{P_R}{P_F}}{1-\frac{P_R}{P_F}} \qquad \text{or} \qquad \beta_{Undercoupled} = \frac{1-\frac{P_R}{P_F}}{1+\frac{P_R}{P_F}} \quad (5)$$

E is the cavity gradient in MV/m, I_0 is the beam current in Amperes, L is the cavity length of 0.5 m for standard CEBAF cavities and 0.7 m for SL21 and FEL3, the loaded-Q (Q_L) of the cavity is approximately $6\text{x}10^6$, f_0 is the frequency of the cavity, δf is the difference between the RF source frequency and that of the cavity, I_0 is the beam current, and the shunt impedance of the cavity, (r/Q), is 960 Ω/m for both the standard CEBAF cavities as well as those used in FEL3 and SL21.

For CEBAF cryomdodules $\beta >> 1$ and equations (1) and (2) reduce to equations (6), (7). Additionally, with no beam current equation (3) reduces to equation (8).

$$P_{Klystron} = \frac{E^2}{4Q_L} * \frac{L}{(r/Q)} \quad (6)$$

$$P_{Klystron} = \frac{1}{4Q_L} \left(E + IQ_L (r/Q)\right)^2 * \frac{L}{(r/Q)} \quad (7)$$

$$P_{Klystron} = \frac{1}{4} * Q_L * E^2 * \left[\left(\frac{1}{Q_L}\right)^2 + \left(2\frac{\delta f}{f}\right)^2 \right] * \frac{L}{(r/Q)} \quad (8)$$

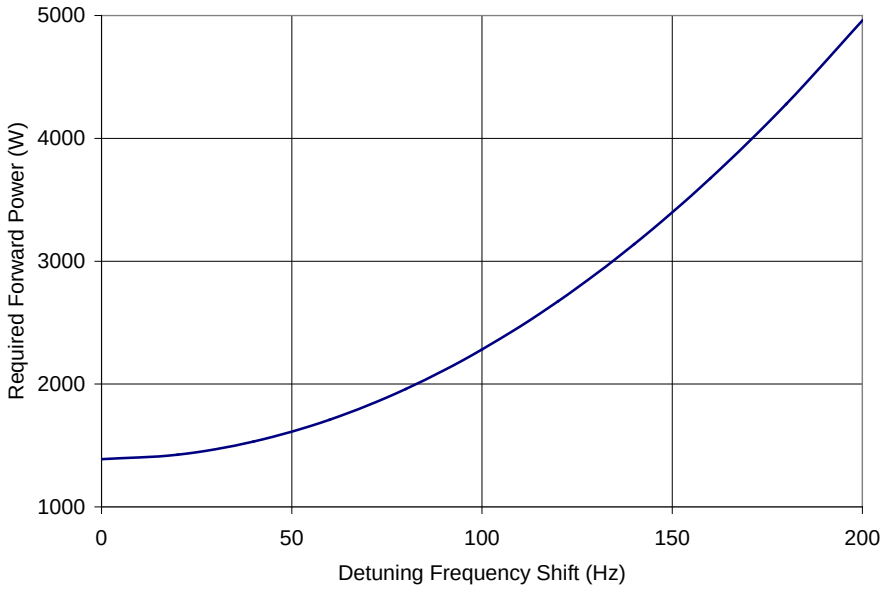

Figure 1. Klystron power required to drive a detuned cavity as a function of detune frequency (δf). For the purposes of the graph the cavity gradient is 8 MV/m, $Q_L = 6\text{x}10^6$ and the frequency is 1497 MHz.

During normal operation, there needs to be a power margin in order to avoid saturation effects in the klystron which cause the control system to oscillate. The linac energy management program (LEM) used in CEBAF budgets approximately 300 Watts for a combination of the klystron power margin and power required to control microphonics effects.

Figure 1 is an example of the power required as a function of detuning for a five-cell cavity which has $Q_L = 6\text{x}10^6$ (a bandwidth of 250 Hz), a gradient set point of 8 MV/m, and no beam loading. For a cavity with these characteristics, 300 Watts of detuning is approximately 55 Hz.

Experimental Setups

General

In general the experiments made use of an RF switching network and combiner to apply a secondary RF source to the klystron drive signal. Several layers of interlock were used to insure that we did not risk damaging the window structures by driving high power RF into the system for more than 250 ms under a fault condition. The original configuration allowed us to inject an open loop 1497 MHz RF signal into the cavity. After the preliminary results were reviewed, the test system was modified so that we could apply closed loop control around the cavity gradient or phase using the secondary source.

Test setup open loop control

The open loop test setup is shown in Figure 2. The system made use of an Agilent E4424B RF signal source and a Wavetek 801 pulse generator. The signal source was configured as an open loop phase and amplitude control RF source. The test setup allowed one to inject a secondary pulse of RF into the LLRF drive signal path after an adjustable delay time. The timing of the pulse and the pulse delay were controlled using the pulse generator. The secondary interlock which restricted application of the secondary RF source to 250 ms duration was provided by a custom designed PCB triggered by the arc detector fault signal. It removed the permit signal after a delay, which was set by adjusting jumpers on the PCB. Additionally, the long vacuum fault was used to disable the LLRF drive signal after the waveguide vacuum exceeded 1e-7 Torr for more than 5 seconds. An additional, unintended, interlock was the "gradient present in RF OFF state" interlock. This interlock shut off the klystron high voltage source when the gradient was above 1 MV/m for more than approximately 50 ms after an arc.

Test setup closed loop gradient control

A similar test setup was used for closed gradient loop control. It is shown in Figure 3. In this instance a second Wavetek 801 pulse generator was used to establish the set point for the gradient. A Stanford Research SR560 amplifier was used to amplify the error signal which was the difference signal between the output of the pulse generator and the transmitted power signal from the crystal detector. The typical gain and bandwidth settings were 5000 and 100 kHz respectively. The variable rise time feature of the pulse generator allowed us to set the target gradient rise time between 5 ns and 200 ms. The values of 10 ms and 100 ms were chosen for the experiment. The RF source AM modulation settings were 100% modulation, external input. The power level was adjusted in order to reduce the maximum drive signal to the klystron.

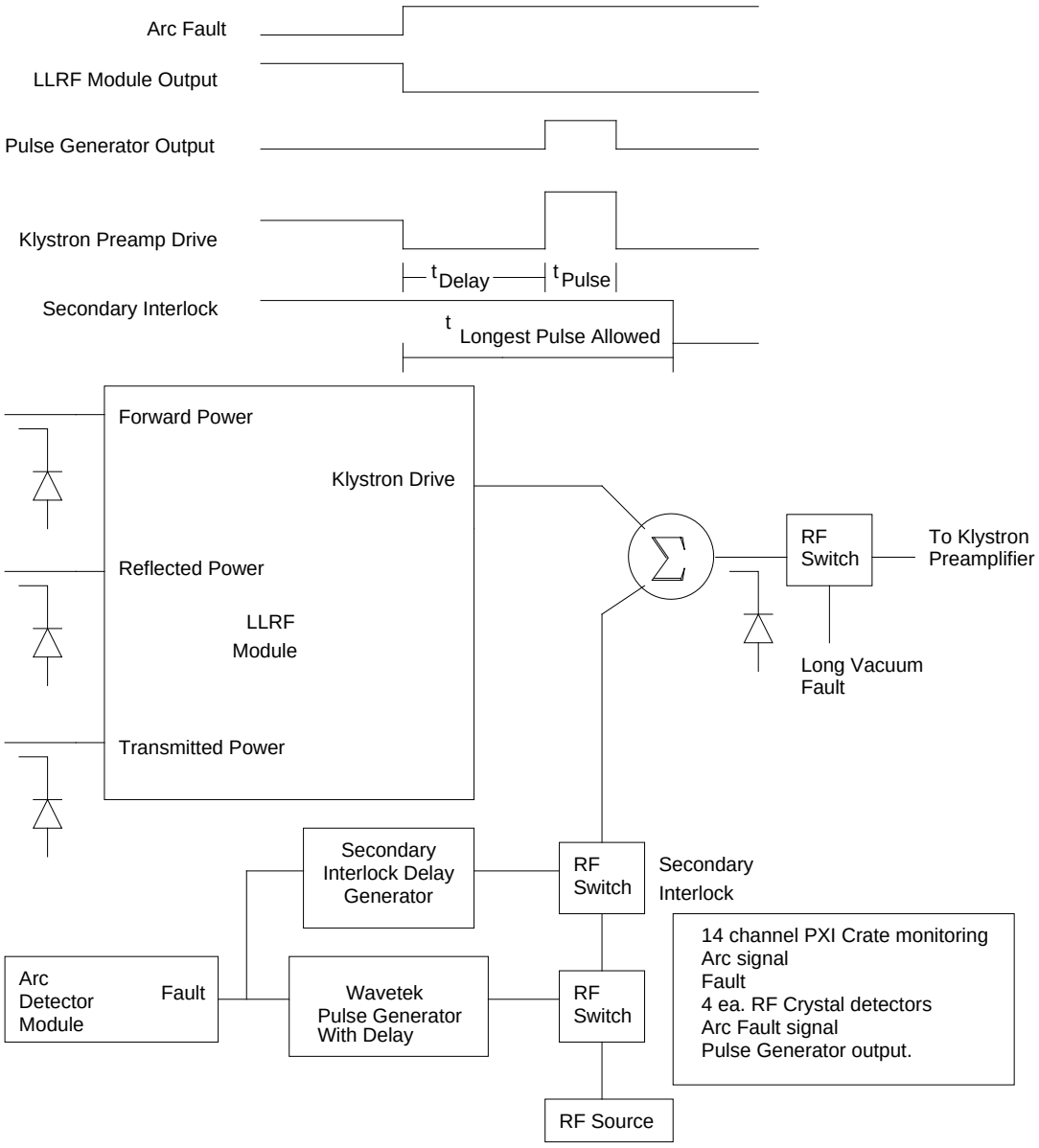

Figure 2. Test setup for Open loop control

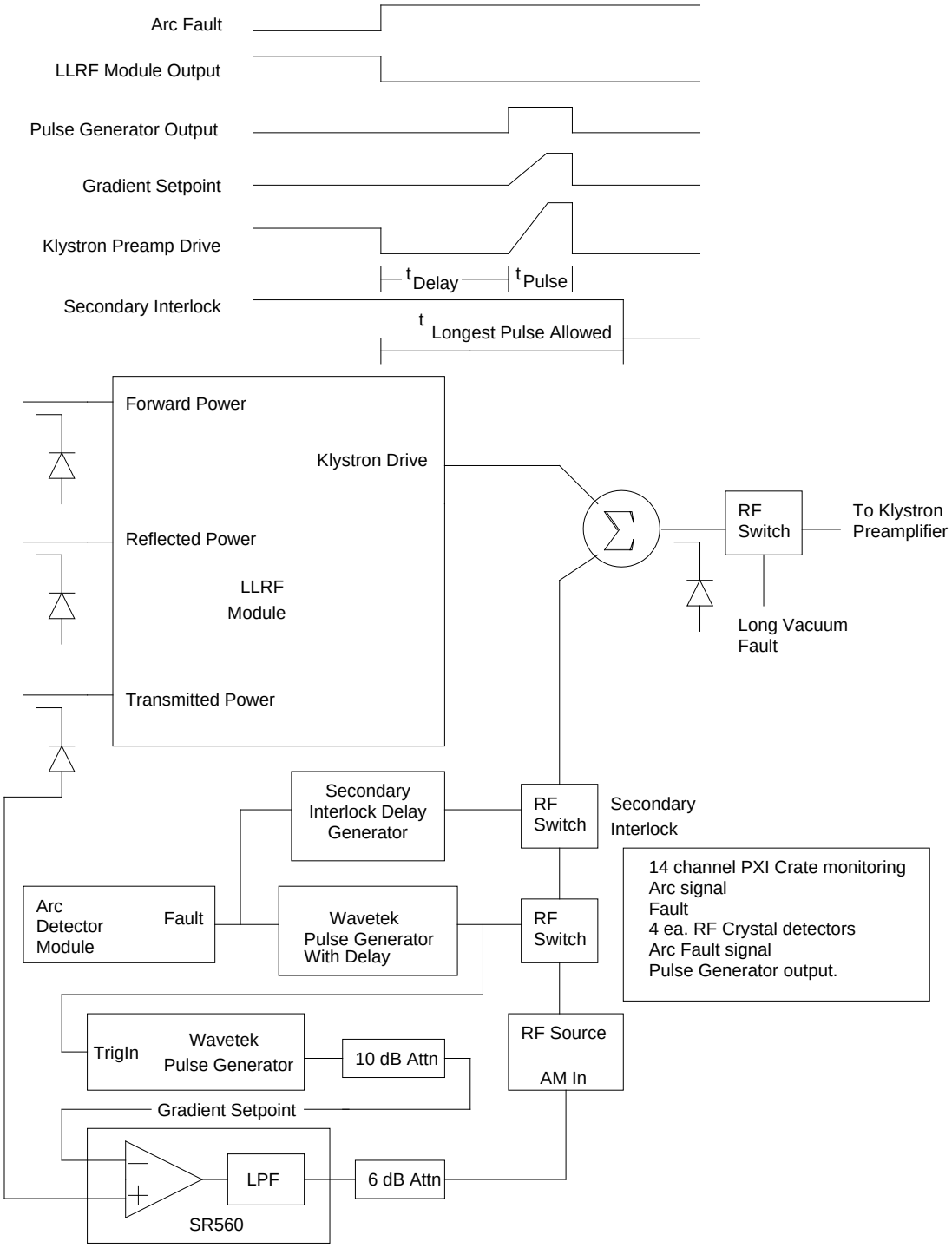

Figure 3. Test setup for Closed loop amplitude control

Test setup for closed loop frequency control

The test setup shown in Figure 3 was modified such that the RF source acted as a voltage controlled oscillator – phased locked loop (VCO-PLL). The block diagram is shown in Figure 4. Additionally, a resonance monitor [9] was added to measure the time domain frequency shifts of the cavity. The output voltage of a resonance monitor is proportional to the frequency difference between the test signal, in this case the cavity transmitted power, and a reference source. The initial test in this configuration was to remove the RF drive signal for 10 ms to 20 ms and observe the transients in the cavity frequency. The zone FSD signal was used as an interlock that removed RF drive in the event there was a fault during the test. Additionally, this configuration was used to measure the spectrum of the background modulation as well as the dynamic Lorenz force detuning coefficient [9]. During the latter test the gradient was set to 5 MV/m. The resonance monitor was then tuned to the cavity to reduce the DC offset in the output signal. The tracking generator output of an Agilent model 35670A dynamic signal analyzer was applied to the AM modulation input of the cavity drive RF source and the gradient was modulated plus and minus 0.5 MV/m. The magnitude of the RF resonant frequency shift as a function of AM frequency was then recorded by the dynamic signal analyzer.

A second VCO-PLL configuration was use that is shown in figure 5. In this test the LLRF system was used to drive the cavity until such time as an arc occurred. Just as in the first tests the RF is restored after 10 ms to 20 ms. However, in this test the frequency of the RF is controlled rather than the amplitude. Again the resonance monitor was used to record the cavity frequency transients associated with the event. The signals were digitized and recorded using a long record length oscilloscope.

Data Acquistion

Crystal detectors were used to record the RF power levels for the forward, reflected, transmitted and drive signals. They were characterized by injecting an RF signal into each detector and recording the resultant voltages. The voltage readings recorded during the test were converted to RF power levels using these data along with reference levels extracted from the EPICS archiver. The crystal detector voltage waveforms recorded during the open loop and closed amplitude loop measurements were converted to RF power levels for the open loop and closed amplitude loop measurments. Since the primary purpose of the closed loop frequency measurements was the frequency shifts associated with the transients, the raw crystal detector voltages were presented along with the frequency shift data for this section of the work.

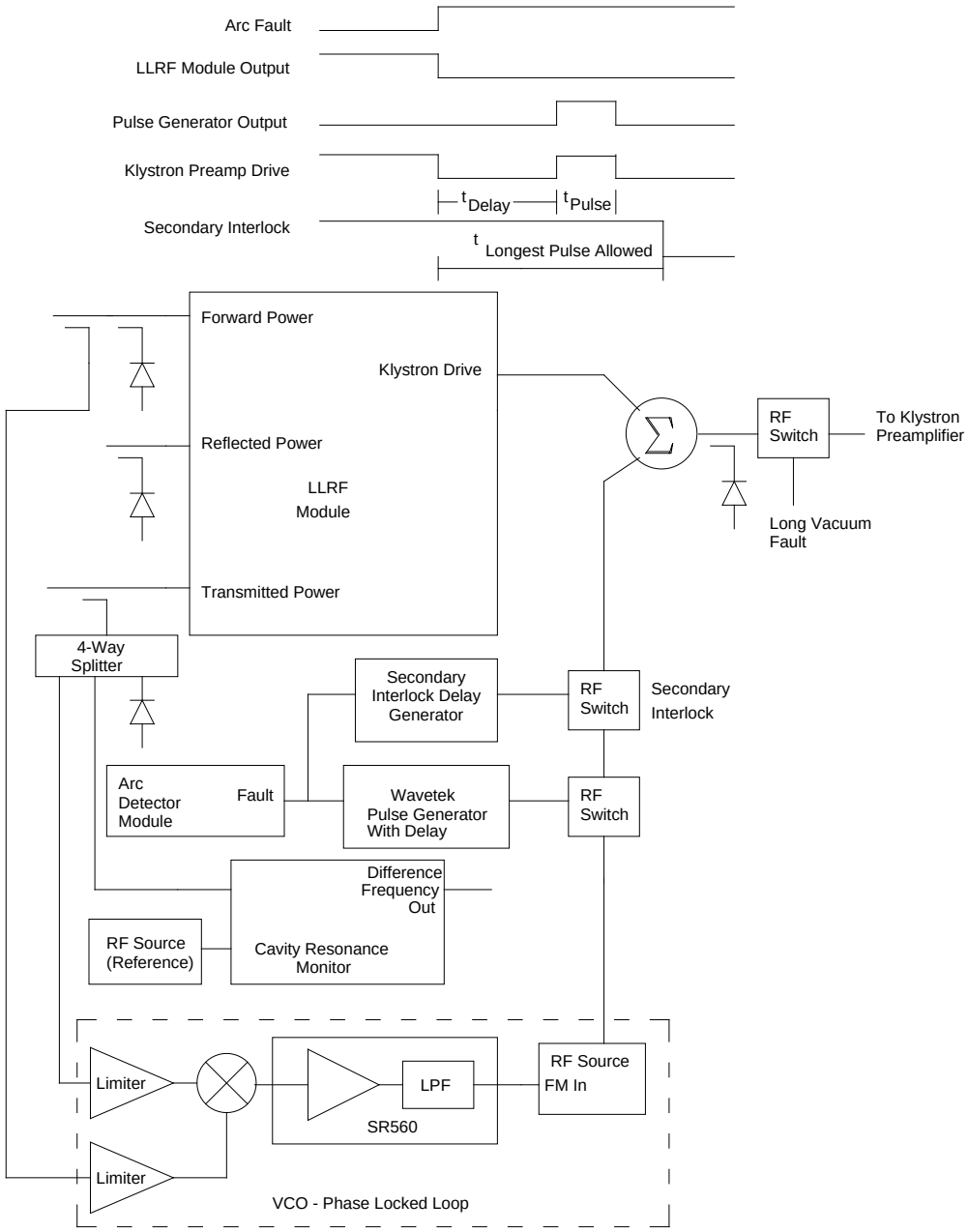

Figure 4. Configuration for arc recovery test which used a VCO-PLL for the secondary RF pulse and a cavity resonance monitor to determine the cavity frequency fluctuations as a function of time.

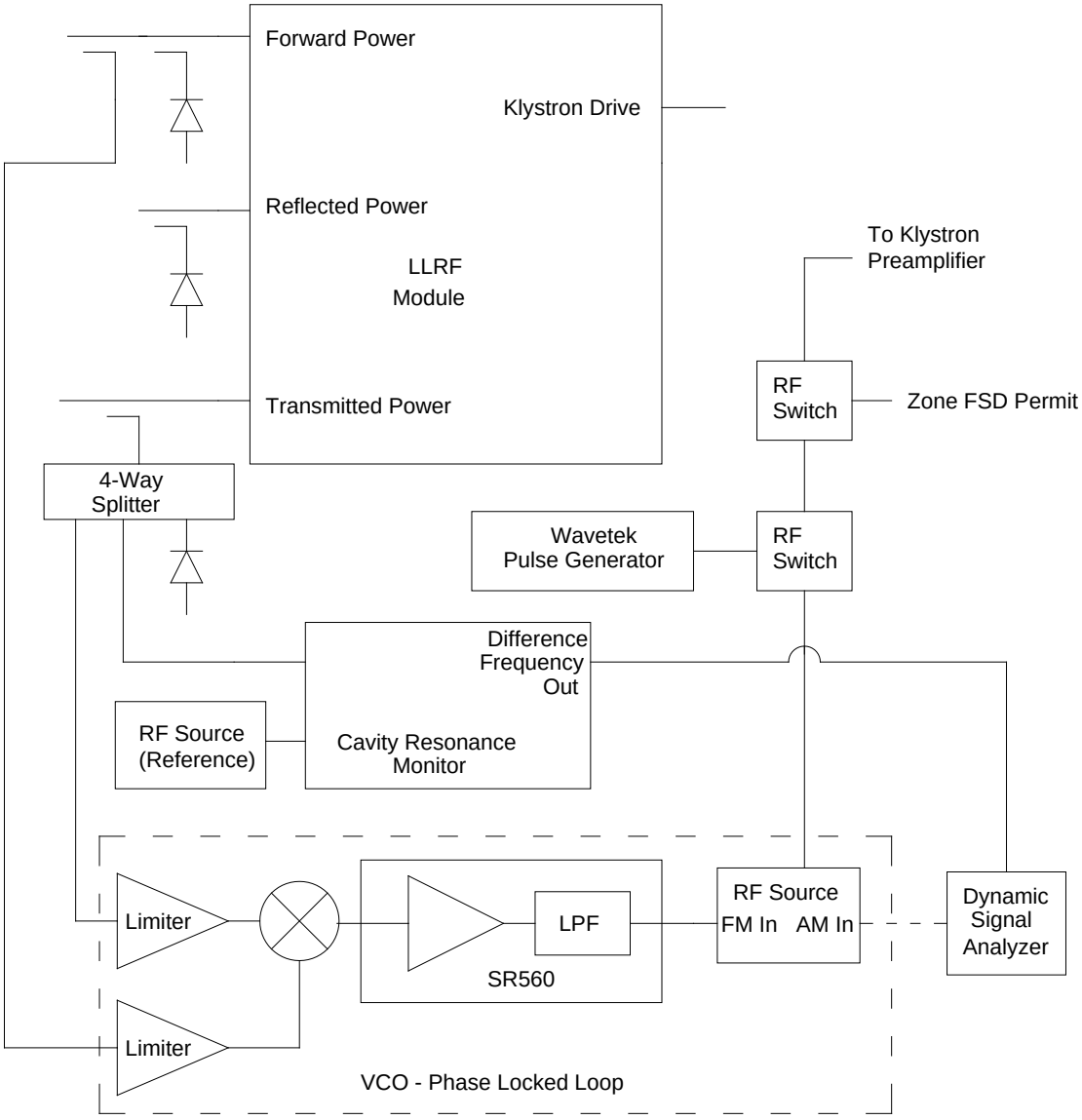

Figure 5. Configuration of VCO-PLL and resonance monitor systems for “Pulsed Off” response test.

Experimental Results

Initial tune-up for Open Loop Control

After the directional couplers were put in place, the cavity was tuned and gradient was established at 6 MV/m. Cavity SL16-5 was selected for this test because it arced every 5 to 10 minutes at this gradient. The voltage of the transmitted power crystal detector was noted. The tuner was set to manual and the LLRF output signal was disconnected from the combiner. The RF state remained on and the gradient was set to a value greater than 2 MV/m. This was done so that the HV interlock would remain valid when the gradient was achieved with the secondary source. The secondary source amplitude and frequency were adjusted while operating the cavity in a single shot pulse mode with a 12 ms pulse.

Open Loop Control

Figure 6 is the waveforms for the forward power, reflected power, gradient, arc and waveguide vacuum signals for the cavity when pulsed open loop with the RF frequency tuned for maximum gradient. The resultant open loop gradient was 5.75 MV/m +/- 0.2 MV/m. A similar process was followed in order to set the amplitude and offset for the gradient set point of the closed loop system. For all of the data the vacuum signal is considered good when the voltage is above the set point of 4.6 V and in a fault mode when it is below 4.6 V. While there is a minor variation in the gradient, the signals demonstrate that on can achieve a relatively stable gradient of 5.75 MV/m in an open loop mode. The fast transients in the reflected power signal at the beginning and end of the RF pulse are typical for an over coupled cavity.

Figure 7 shows the recovery of the gradient after a waveguide vacuum fault. The variations in gradient and reflected power are probably due to microphonics effects. Figure 8 shows the recovery of the gradient after an electronic quench. The transients in the reflected power and gradient are very large and indicate that the frequency of the cavity is being modulated substantially as compared to the bandwidth of the fundamental power coupler which is about 250 Hz. Figure 9 also shows the response of the system after an electronic quench. In this instance the secondary pulse was applied for a longer period of time. The instability in the gradient was present for more than 130 ms. In both these cases the fundamental cause of the microphonics is thought to be the sudden loss and reestablishment of the Lorentz force detuning when the gradient is suddenly removed and reestablished. The assumption is that more vibrational harmonics are being excited by the faster transient in cavity gradient associated with the electronic quench. The transient time effects are further analyzed later in this technical note. Note that the negative going signal on the arc detector waveforms for Figures 7 through 9 are an artifact of the diagnostics. More typical arc detector signals are shown in the remainder of the figures.

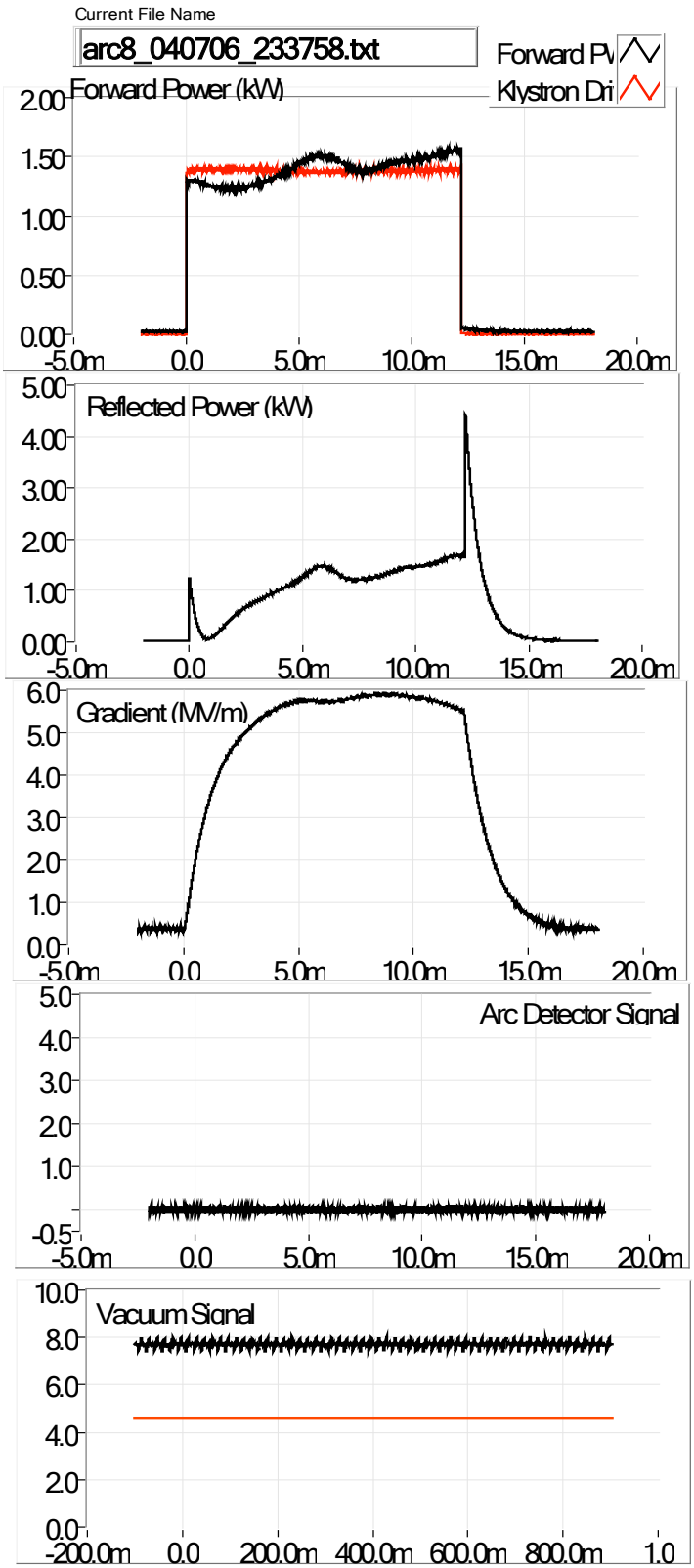

Figure 6. Driving the cavity with the secondary RF source. Open gradient and phase loops.

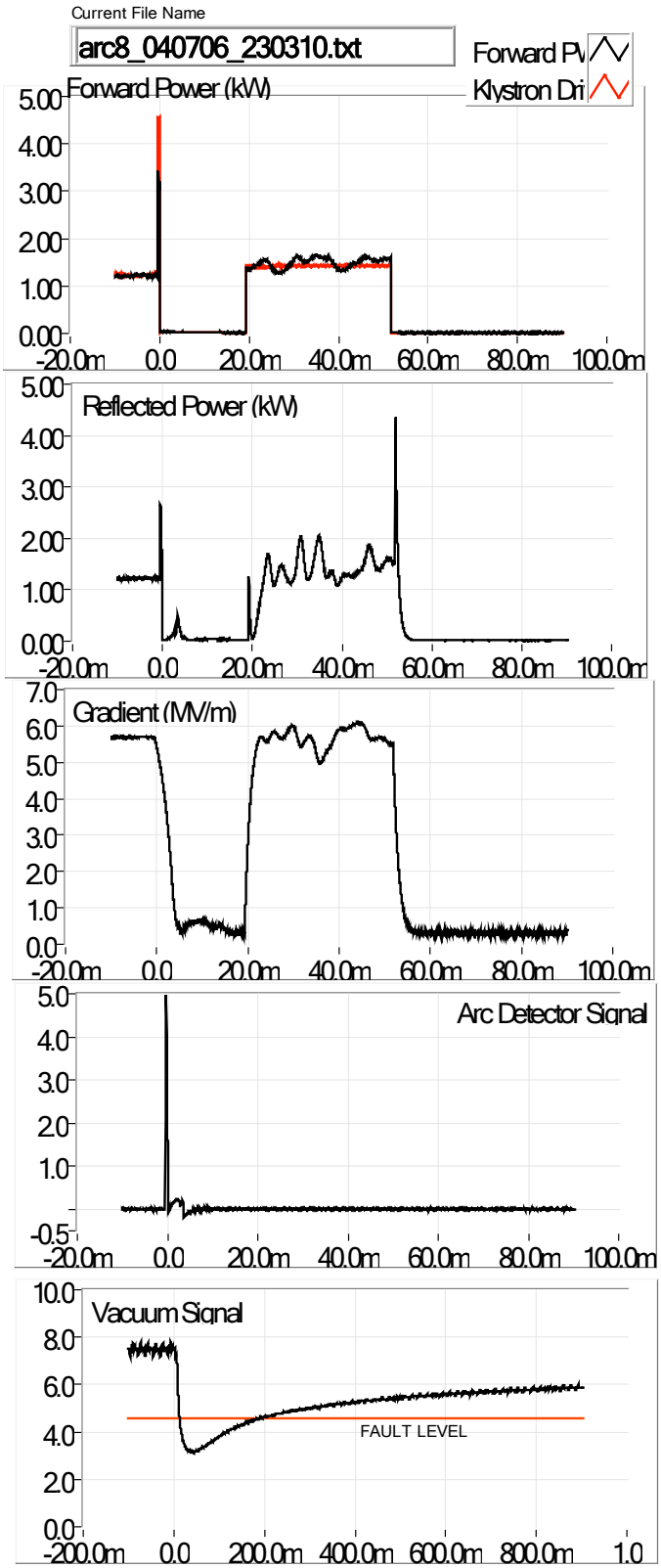

Figure 7. Recovery 30 ms after a waveguide vacuum arc with an open phase and gradient loop. Note the decay time of approximately 8 ms in the gradient.

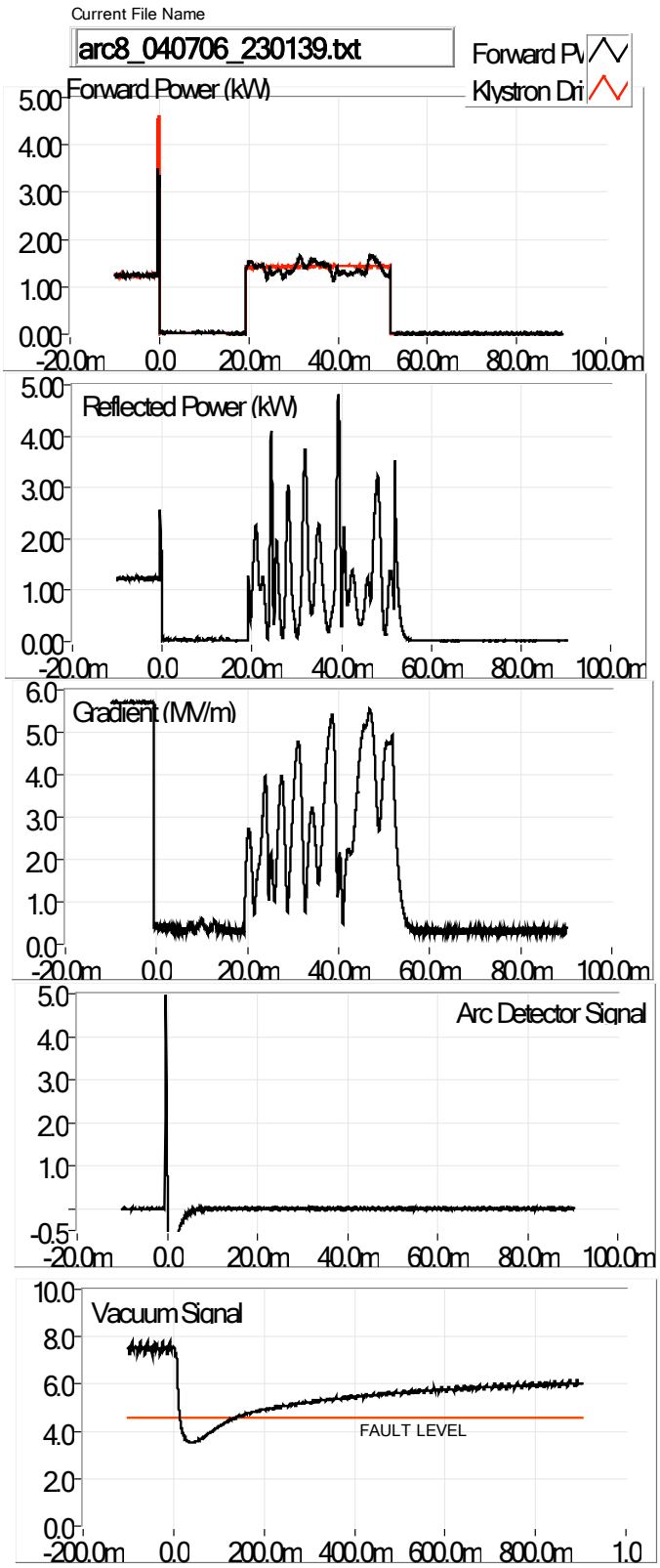

Figure 8. Response of a cavity to an open loop RF pulse applied 20 ms after an electronic Quench. Note that the gradient decays in a few hundred micoseconds.

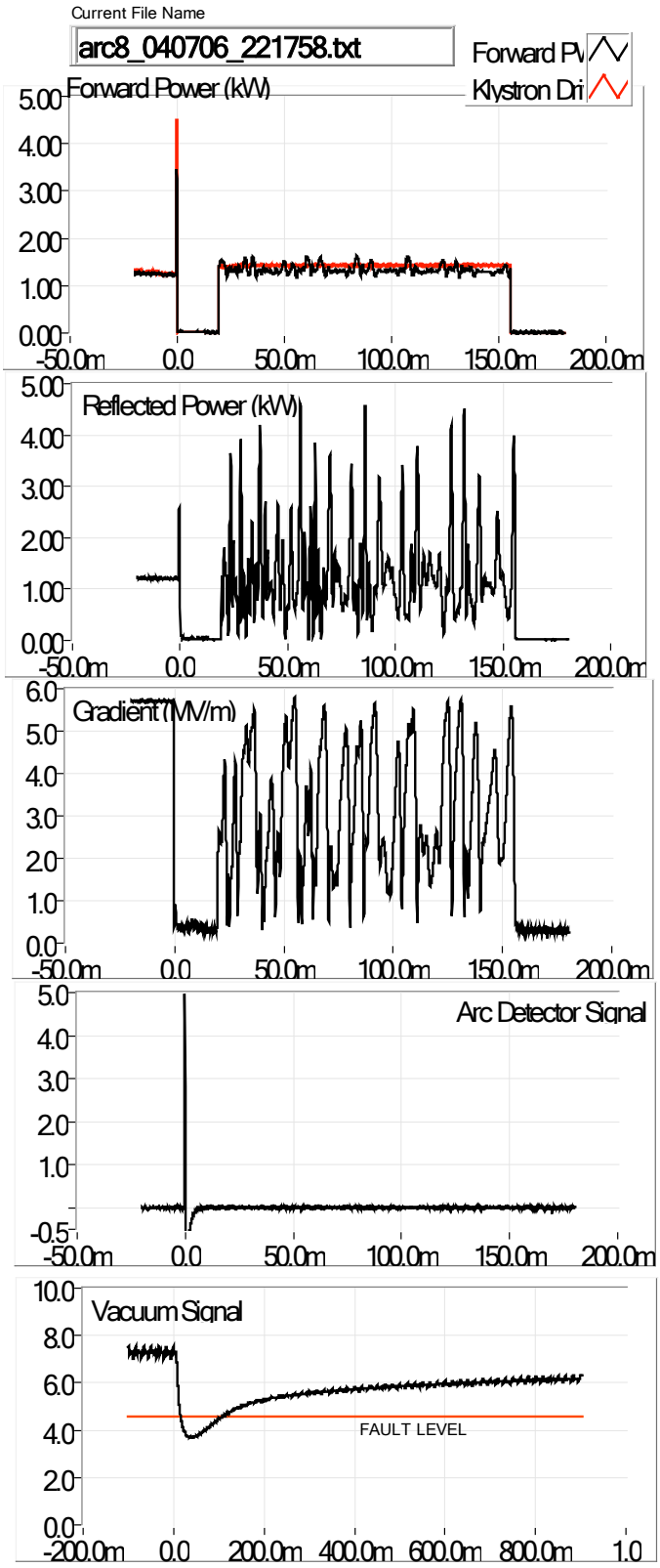

Figure 9. Response of a cavity to an open loop RF pulse applied 20 ms after an electronic Quench. Note cavity still not recovered after 150 ms.

Closed Amplitude Loop Control

Three types of data were taken using the closed amplitude loop controls. In the first data set the rise time was set to 10 ms. The delay time was set to about 20 ms and the gradient was set to 6 MV/m. Figure 10 is the waveforms for closed loop operation at 6 MV/m with no preceding fault. Figure 11 is the waveforms for closed loop recovery after a waveguide vacuum fault. The transients in the forward power are present because the control loop is varying the drive signal in order to maintain constant gradient while the frequency is being modulated by microphonics-driven detuning. Figure 12 is the waveforms for closed loop recovery after an electronic quench. 25 ms after the cavity is turned off the forward power is restored. The cavity gradient, forward power and reflected power signals oscillate substantially for about 10 ms. About 30 ms after the initial arc event the cavity arced again. The discharge was sustained by the forward power for the remaining 20 ms of the forward power pulse. During this time approximately 1 kW of RF power (10 J) is delivered to the discharge. While this amount of energy may seem excessive it is comparable to the 5 J of stored energy which normally is transferred from a 5-cell cavity operated at 5 MV/m to a discharge during a waveguide vacuum arc. It should be noted that the vacuum recovery time for this event was 2 seconds which is much longer than the nominal 250 ms associated with a waveguide vacuum arc.

In the second set of data the rise time was set to 10 ms. The delay time was set to about 20 ms; the gradient was set to 1.75 MV/m; and the secondary pulse width was increased to 150 ms. Figure 13 is the waveforms for closed loop operation at 1.75 MV/m with no preceding fault. Figure 14 is the waveforms for closed loop recovery after a waveguide vacuum fault. Again, the transients in the forward power are present because the control loop is varying the drive signal in order to maintain constant gradient while the cavity frequency is being modulated by microphonics-driven detuning. Figure 15 shows the response of the system to an electronic quench. Again there are excessive transients in the forward power as the system tries to maintain gradient in spite of the excessive microphonic oscillations. The cavity did not arc during this event because the target gradient was much lower. Additionally, it appears that the microphonic oscillations were starting to decay by the end of the 150 mS secondary pulse.

Figures 16, 17 and 18 show similar results for a target gradient waveform which had a 100 ms rise time. The significant results for this test are that the electronic quench event shown in figure 18 did not fully recover even with a slower rise time. Additionally, the waveguide vacuum fault had substantial transients in the forward power. In fact, the system required twice the forward power to overcome the microphonics effects and maintain a stable gradient as compared to steady state operations without a turn off transient. See Figure 16.

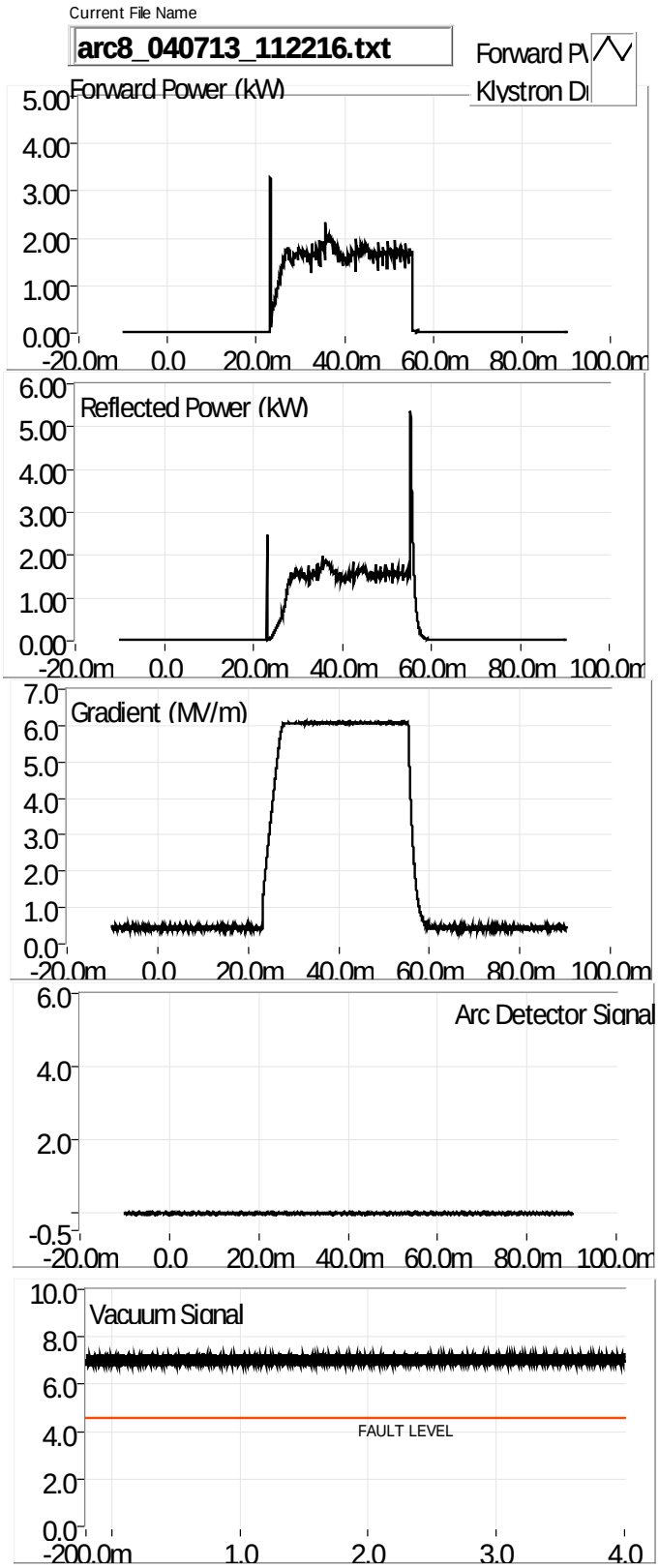

Figure 10. Closed loop control of gradient. Single pulse applied cavity was off prior to event.

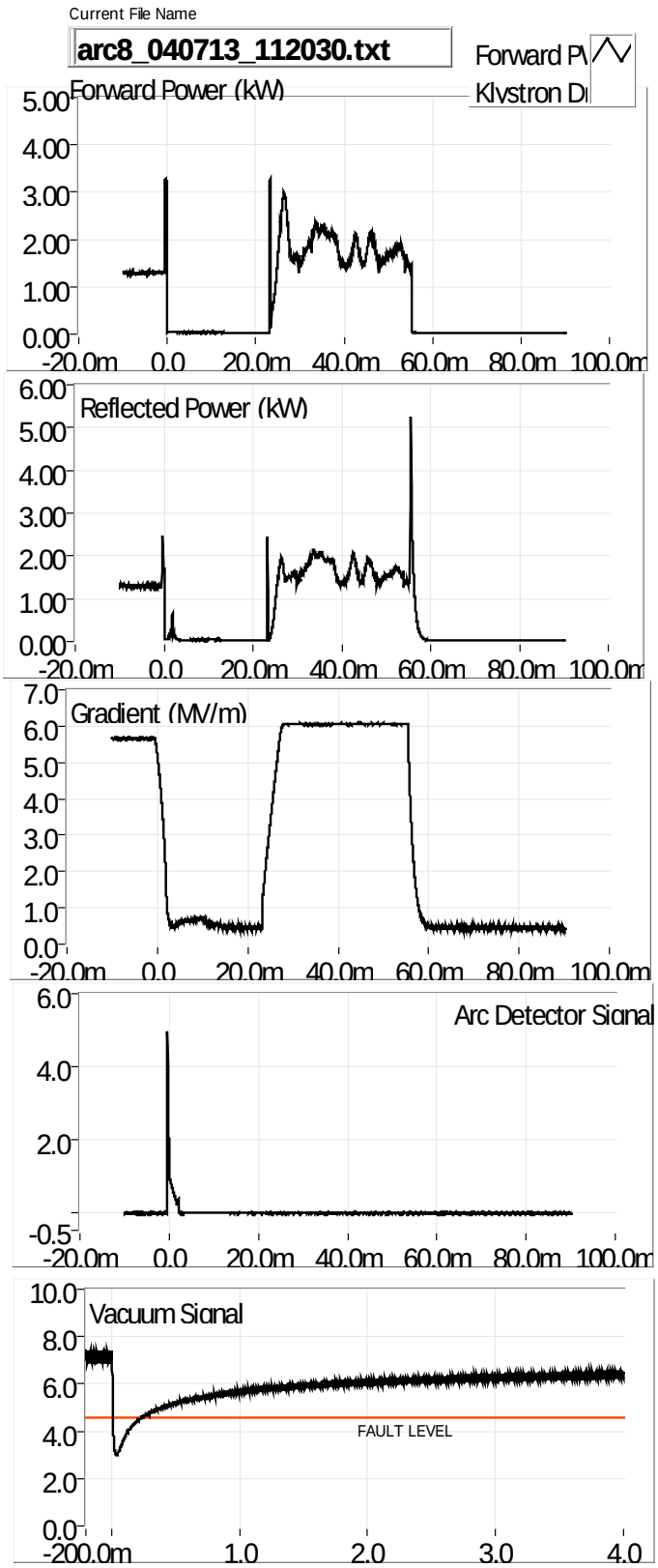

Figure 11. Waveguide Vacuum fault recovery with closed gradient loop.

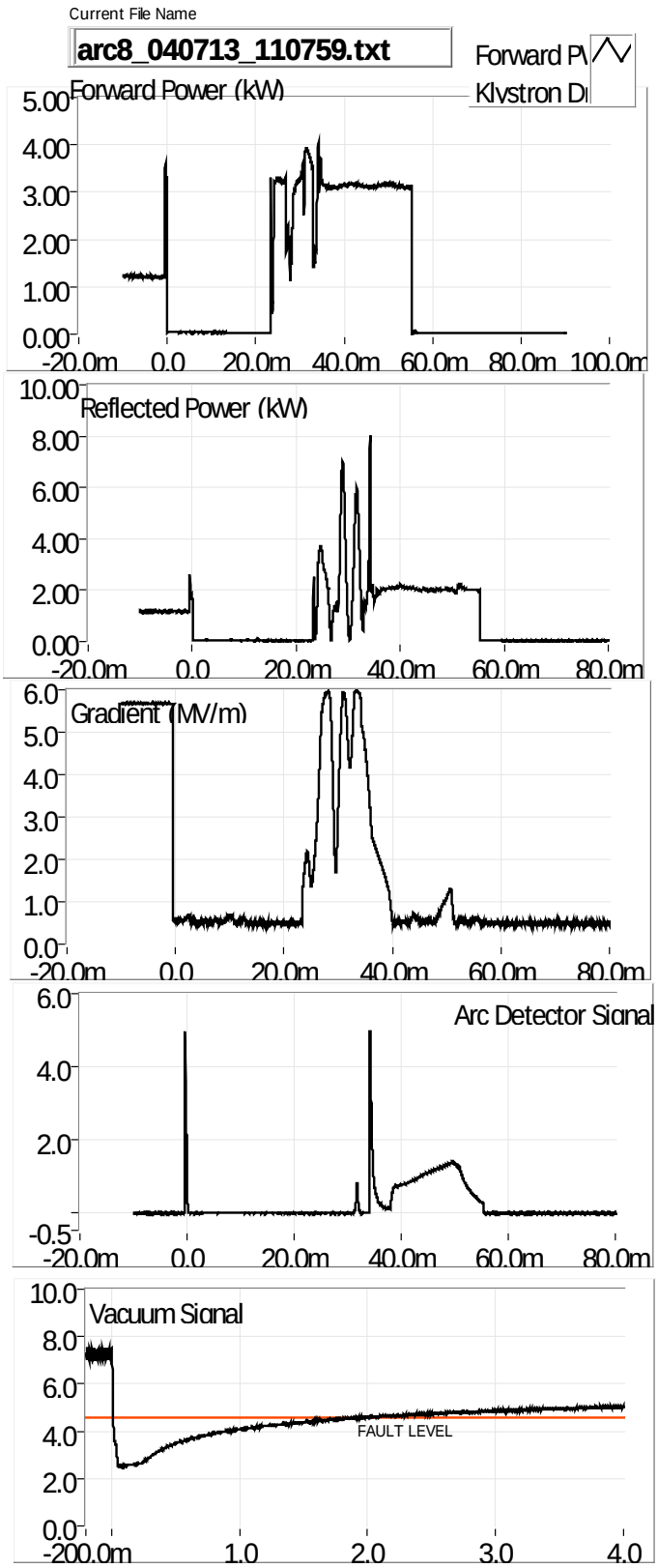

Figure 12. Electronic Quench with a closed gradient loop. Excess forward power lead to a secondary arc. Note the vacuum did not recover for approximately 500 ms.

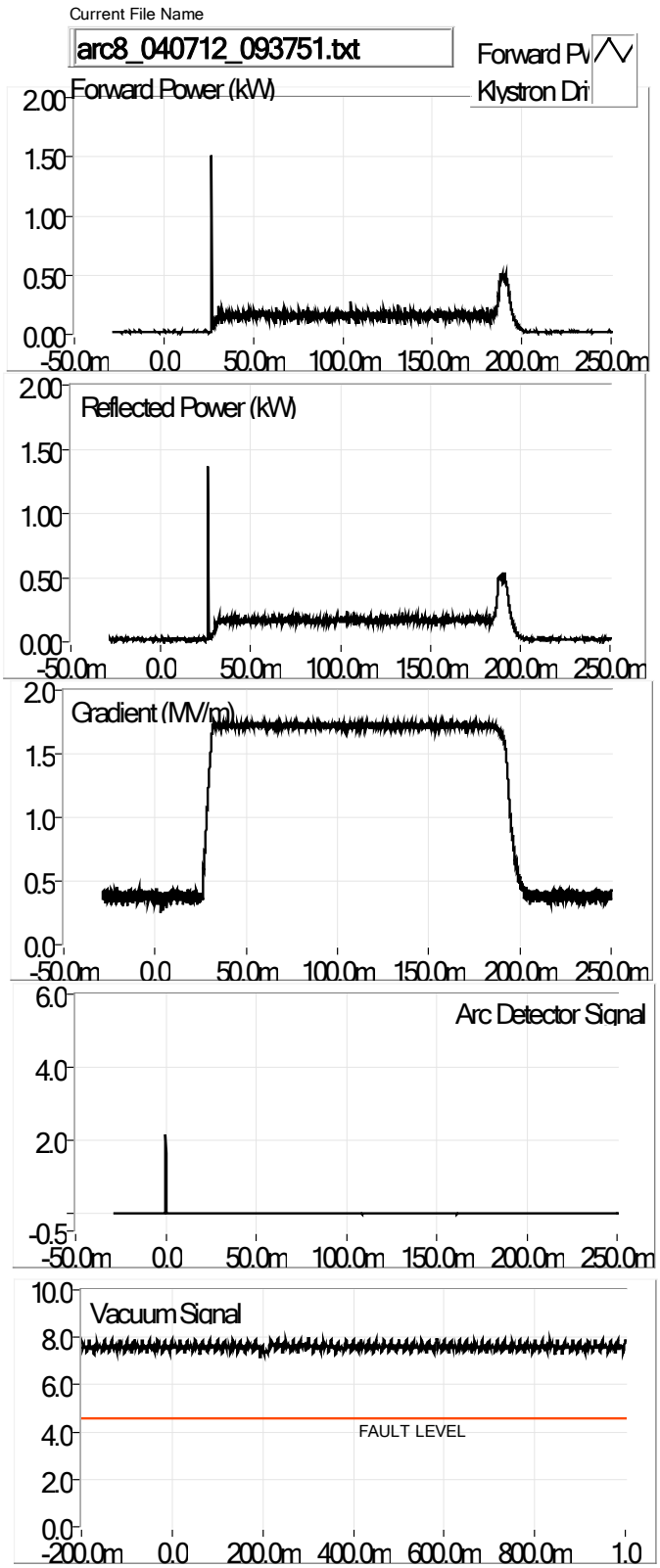

Figure 13. Closed Loop operation with a gradient set point of 1.75 MV/m. The arc "event" was a test pulse. RF was off prior to the pulse.

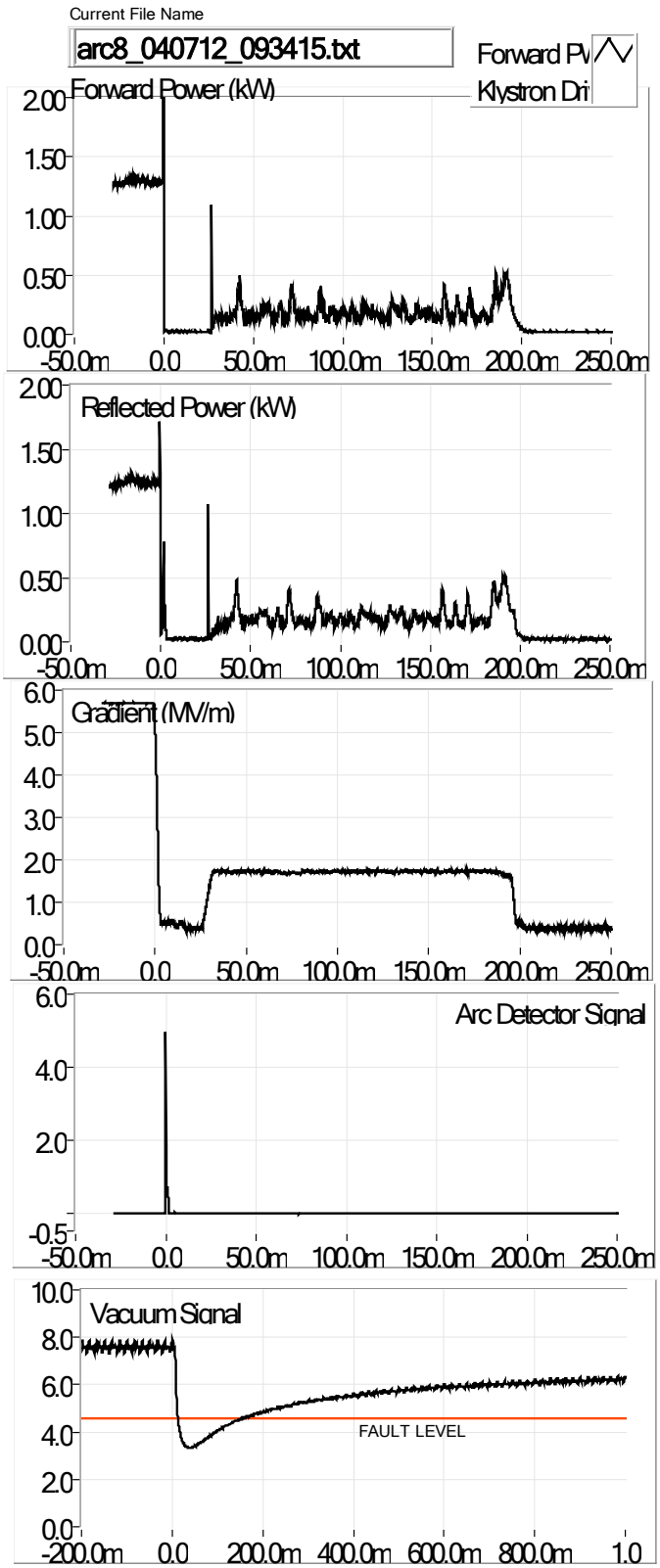

Figure 14. Closed gradient loop operations. Recovery from 6 MV/m to 1.75 MV/m after a waveguide vacuum fault. The pulse at the end of the forward power is an effect of the test setup.

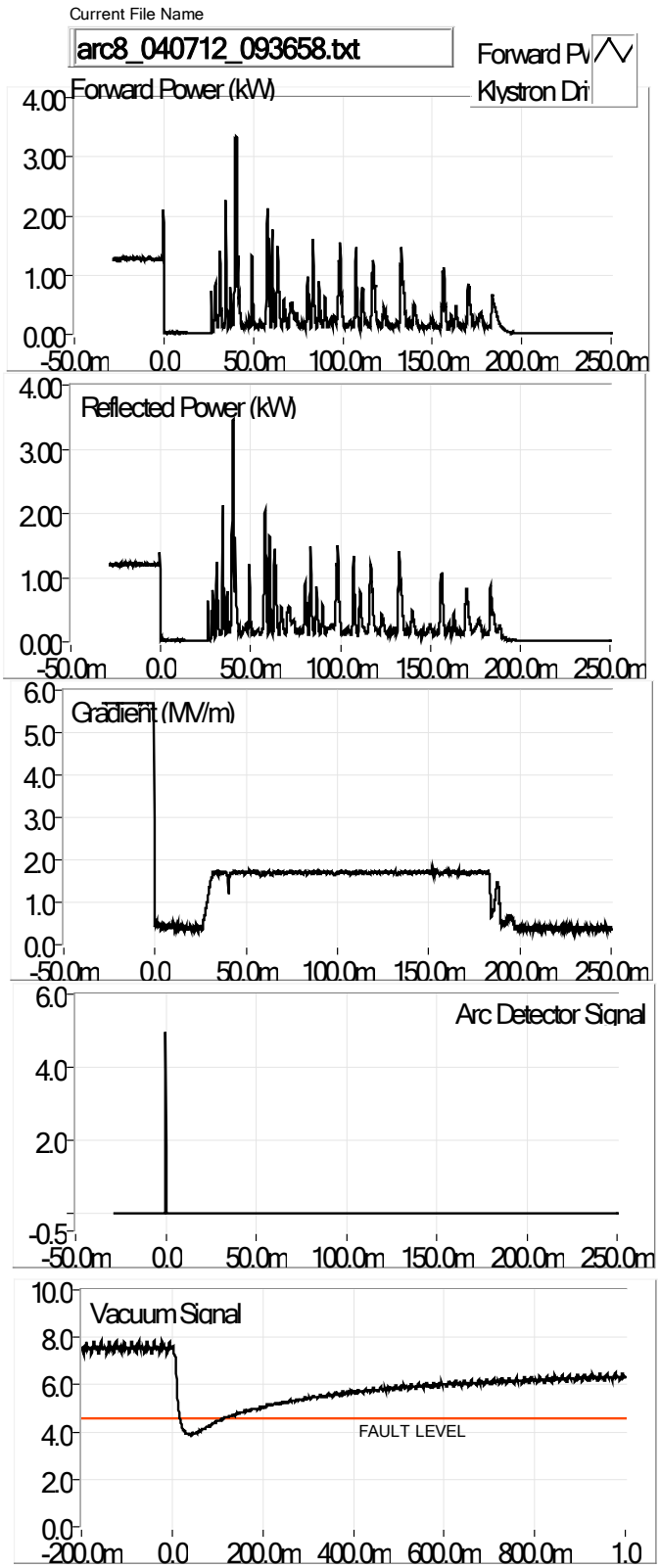

Figure 15. Electronic Quench with closed gradient loop operation at 1.75 MV/m. Duration of second pulse was about 150 ms. Note reduction in forward power variations which indicates that the mechanical oscillations diminishing.

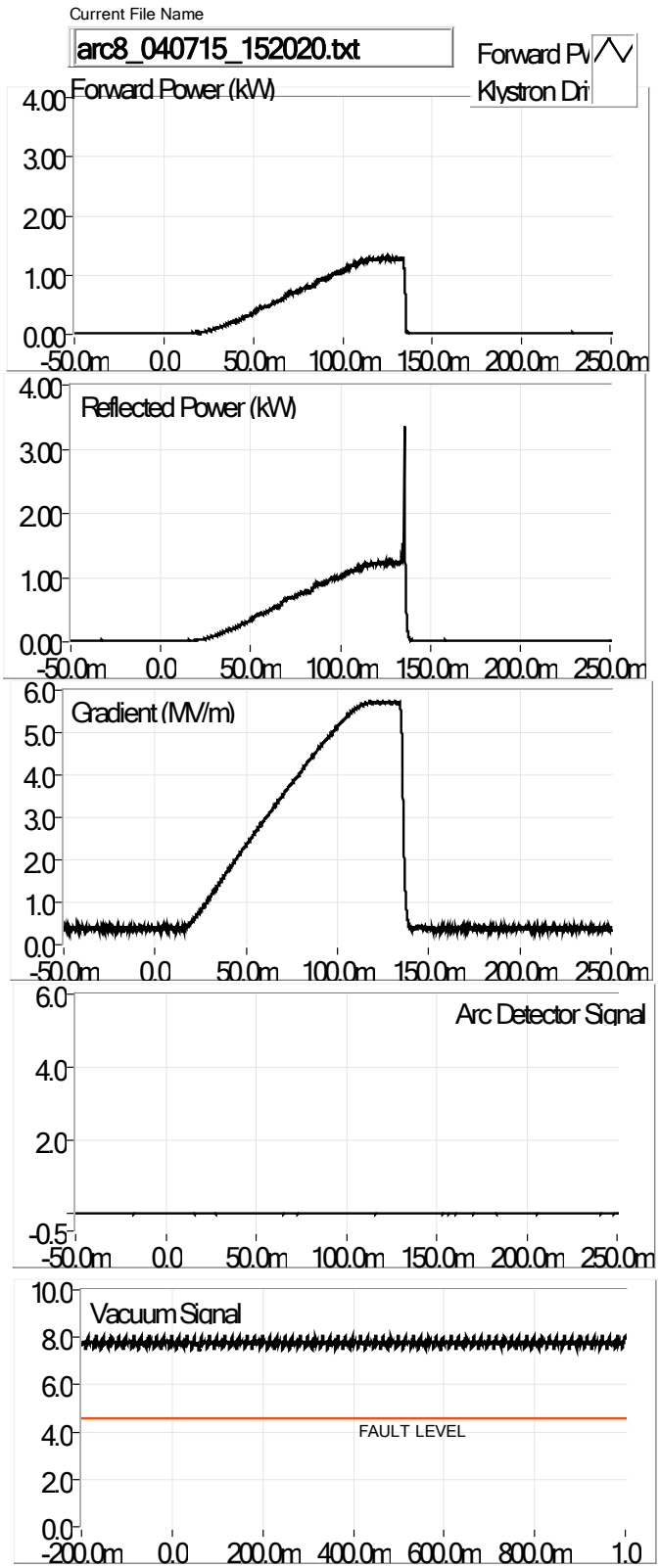

Figure 16. Test pulse with a soft start. Gradient feedback loop closed.

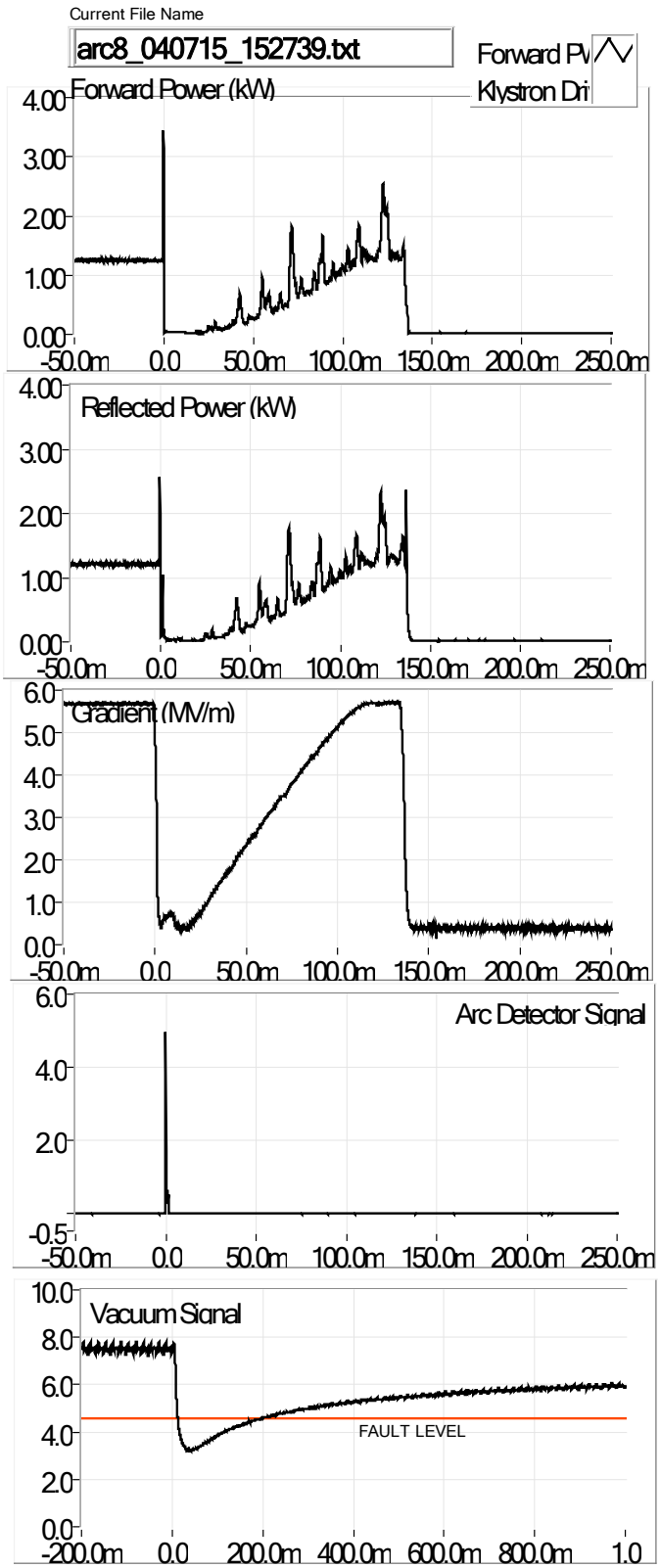

Figure 17. Soft start after a vacuum arc. Note that the microphonics require at approximately twice the power.

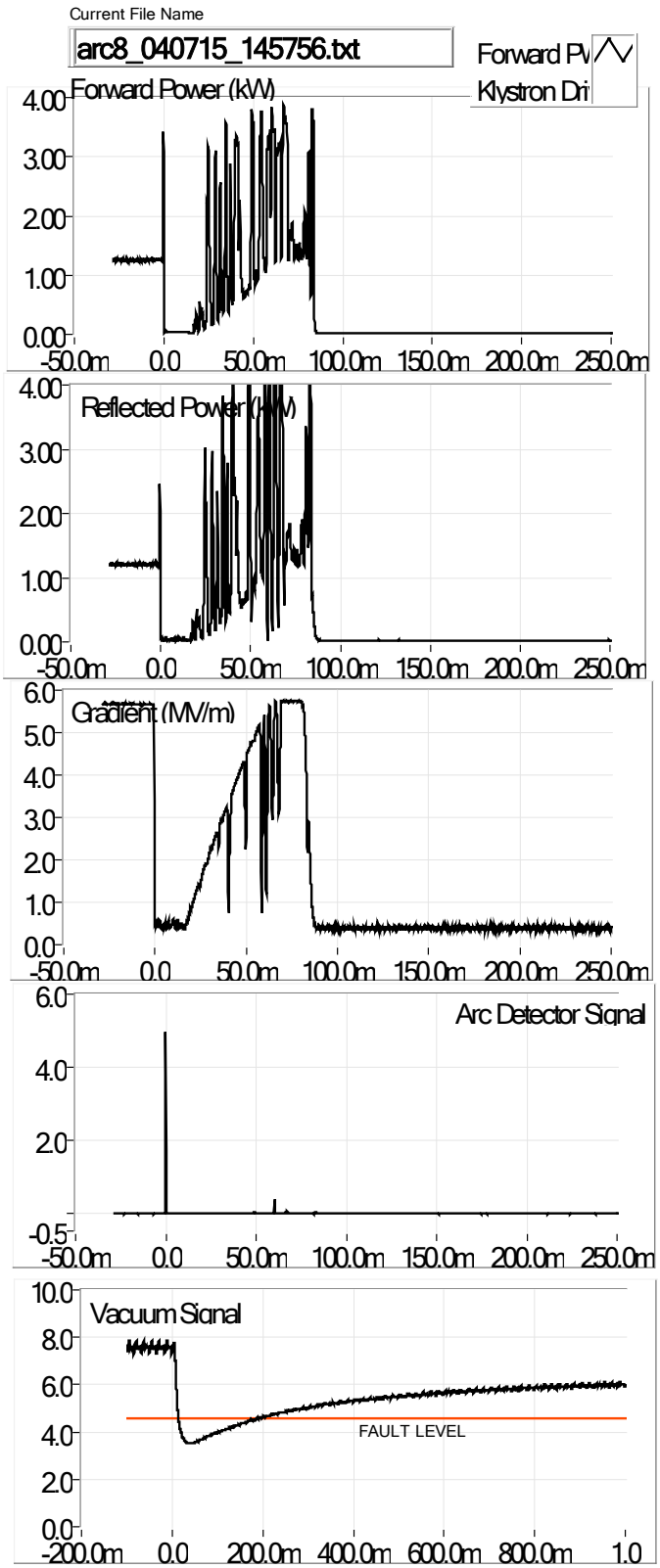

Figure 18. Soft start of after an electronic quench.

Closed Phase Loop Control – Microphonics Measurements

Three types of data were taken with the VCO-PLL based system. The first was the background microphonics of the cavity. For this test the system was configured as shown in Figure 5. The VCO loop was tuned. The gradient was set to 4 MV/m. Additionally, the VCO-PLL loop gain was checked by varying the frequency of the signal source by 200 Hz and measuring the resultant shift in the closed loop frequency. The gain of the loop is ratio of the closed loop frequency shift divided by the change in the source frequency. The measured loop gain was greater than 200. Once this was completed, the frequency of the reference source for the resonance monitor was adjusted to match that of the cavity and the background microphonics data was recorded. This data consisted of 20 seconds of the output of the resonance monitor acquired at 2.5 kS/s. The results of this measurement are shown in Figures 19. The upper graph shows a subset of the time domain data. In it, one observes the frequency content at or near 58 Hz. The lower graph is averaged FFTs of the entire data set broken into ten subsets of 5000 points each. The peak frequencies of 30, 58, 60, 120, 180, 208 and 300 Hz are annotated.

Next, we measured the dynamic Lorentz coefficient. Lorentz force detuning is the shift in the resonance frequency due to the distortions in the cavity geometry when acted upon by the electrostatic forces caused by the electric and magnetic fields within the cavity. The Lorentz detuning coefficient, k, is defined as the ratio of the resultant frequency shift to the square of the gradient, with units of Hz/(MV/m)^2. For steady state the equation used is:

$$k = \frac{(f_1 - f_2)}{E_1^2 - E_2^2} \tag{9}$$

By amplitude modulating the cavity input RF power, the varying Lorentz pressure will cause the cavity to vibrate at the corresponding AM modulation frequency. We used the dynamic signal analyzer to measure the transfer function between the cavity resonance monitor output (proportional to Hz) and the transmitted power crystal detector output signal which is proportional to E^2 (MV/m)^2. The tracking generator output of the dynamic signal analyzer was connected to the amplitude modulation input of the RF signal source. This was used to modulate the amplitude of the RF drive signal and provide a +/- 20% modulation on the cavity input RF power. The dynamic signal analyzer was then set to sweep the frequency of the tracking source between 10 and 409 Hz, while recording the output of the resonance monitor. The results of this test are shown in Figure 20. The upper graph is the response ratio in dB, given by the following:

$$\text{Response\_Ratio} = 20 * \log\left(\frac{\text{CRM\_Output\_Voltage}}{\text{Crystal\_Detector\_Voltage}}\right) \propto \log\left(\frac{\Delta f}{E_2^2 - E_2^2}\right) \tag{10}$$

while the lower graph is the phase shift in degrees. The peak frequencies of 53, 76, 139, 150 and 208 Hz are annotated. The low frequency portion of the curves converges to the static Lorentz coefficient value, which is known from a separate test. Using this static value as a reference, we can compute the dynamic coefficient at any frequency.

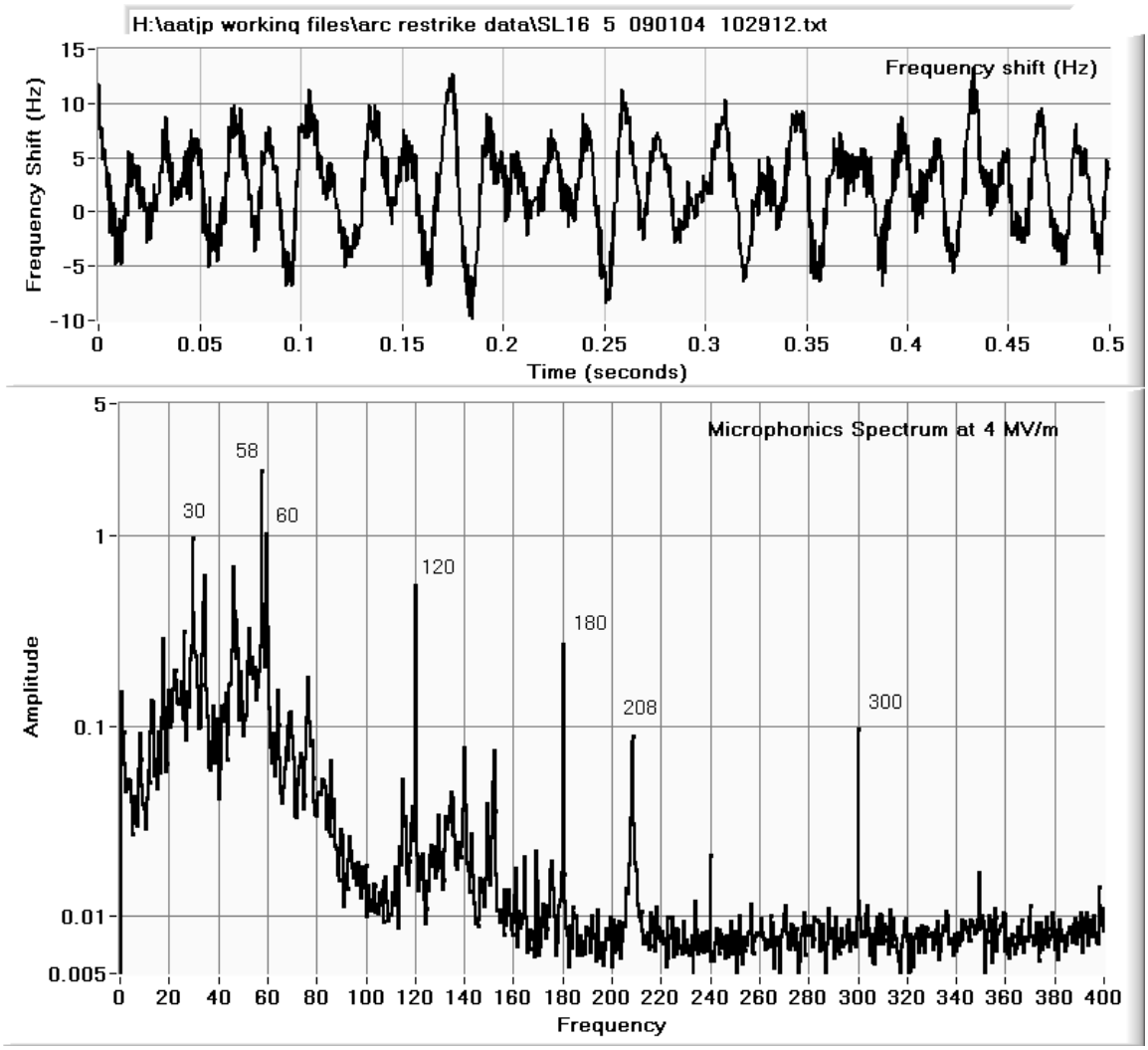

Figure 19. Background microphonics. The spectrum is average the FFT of ten data sets 2 seconds sampled at 2.5 kS/s. The top graph is an expanded view of 0.5 seconds of that data.

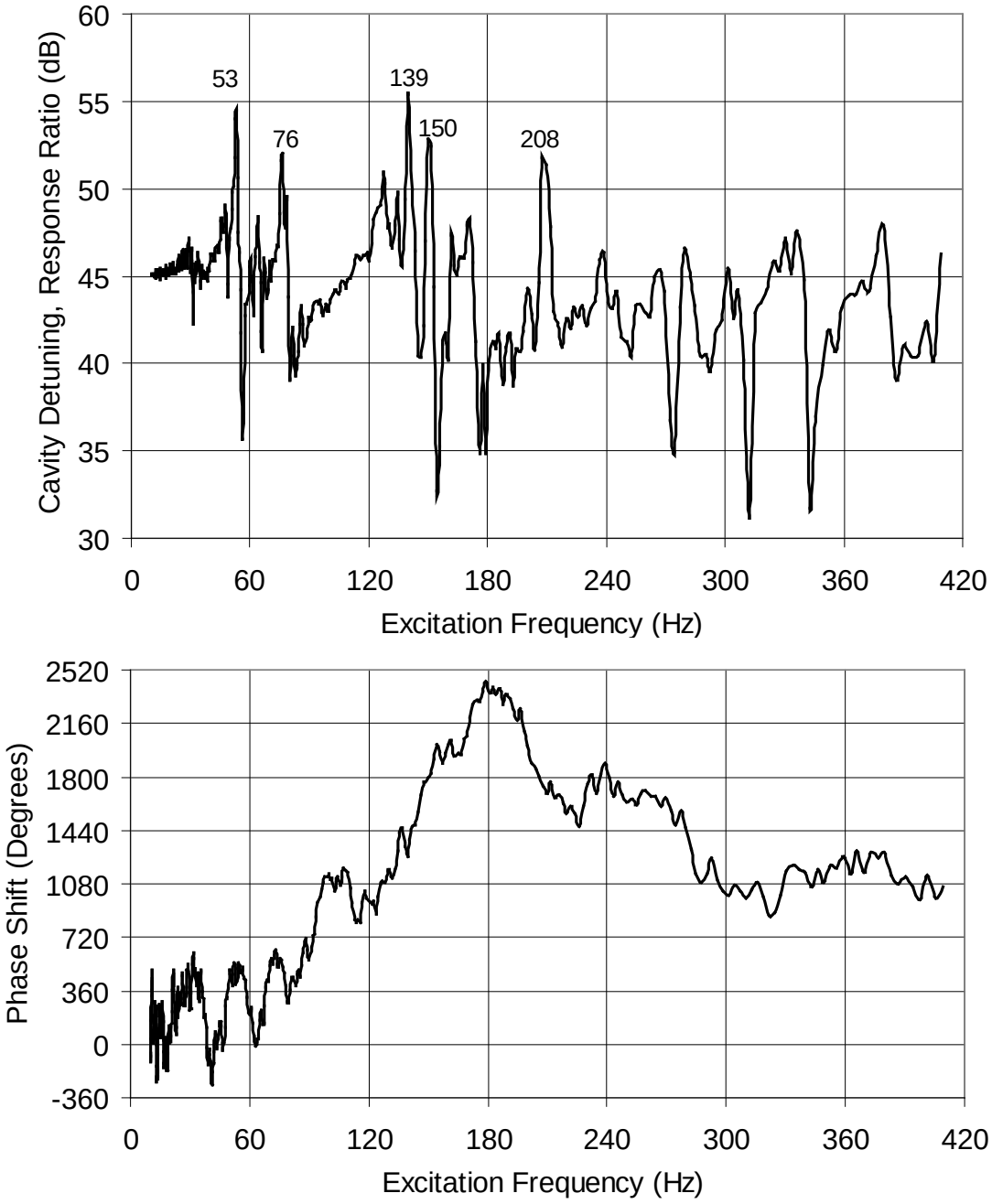

Figure 20. Dynamic Lorenz force detuning response ratio. Forward power modulated +/- 20% which resulted in a +/- 0.5 MV/m variation in cavity gradient at low frequencies.

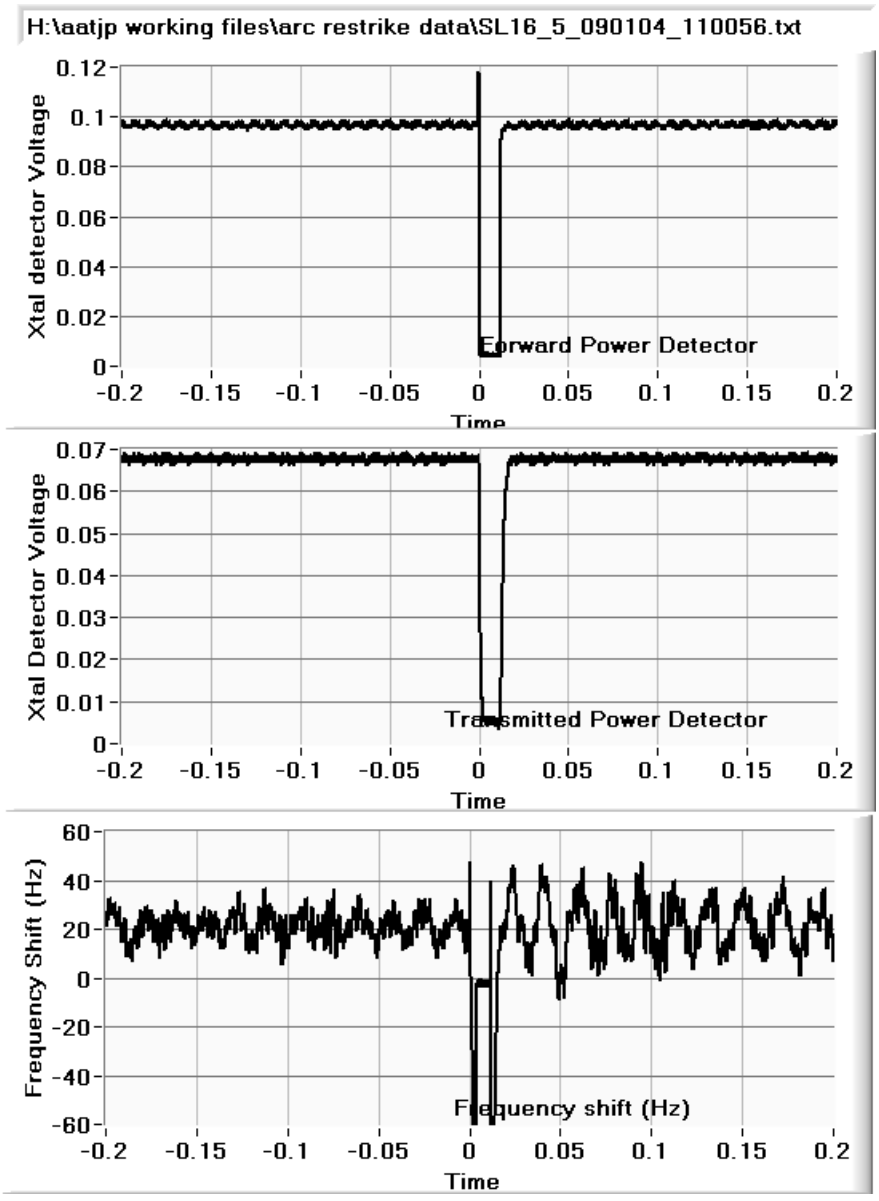

Figure 21. VCO transient response to removal of RF drive for 10 ms. Gradient before and after the pulse was 6 MV/m. The data to the left of zero is the background microphonics. The data to the right of the transient is the combination of the background and the response to the dynamic Lorentz force detuning. The background level was 30 Hz peak to peak. The level was as large 56 Hz peak to peak after the event. The exponential time constant of the cavity field decay and fill were 1 ms and 3 ms respectively.

For the third test using this configuration, a gradient of 6 MV/m was established in the cavity and the drive signal was removed for 10 ms. The frequency fluctuation before and after simple removal of RF power tests, were recorded for 0.5 S and 1.5 S respectively at a sample rate of 250 kS/s. As can be seen in figure 21 the Lorentz force detuning went from the background level of 30 Hz peak to peak to 56 Hz peak to peak after the RF

power was restored. It should be noted that for this data as the remainder of the data that there is a frequency shift transient when the RF is removed and as it is restored which is because of the Lorentz force detuning when the cavity transitions from 6 MV/m to 0 and back to 6 MV/m. Additionally, the CRM is not linear below 1 MV/m, as such the frequency shifts coincident with gradients less than 1 MV/m are not valid. Figure 22 shows a longer duration before and after the event as well as the frequency content before and after the event.

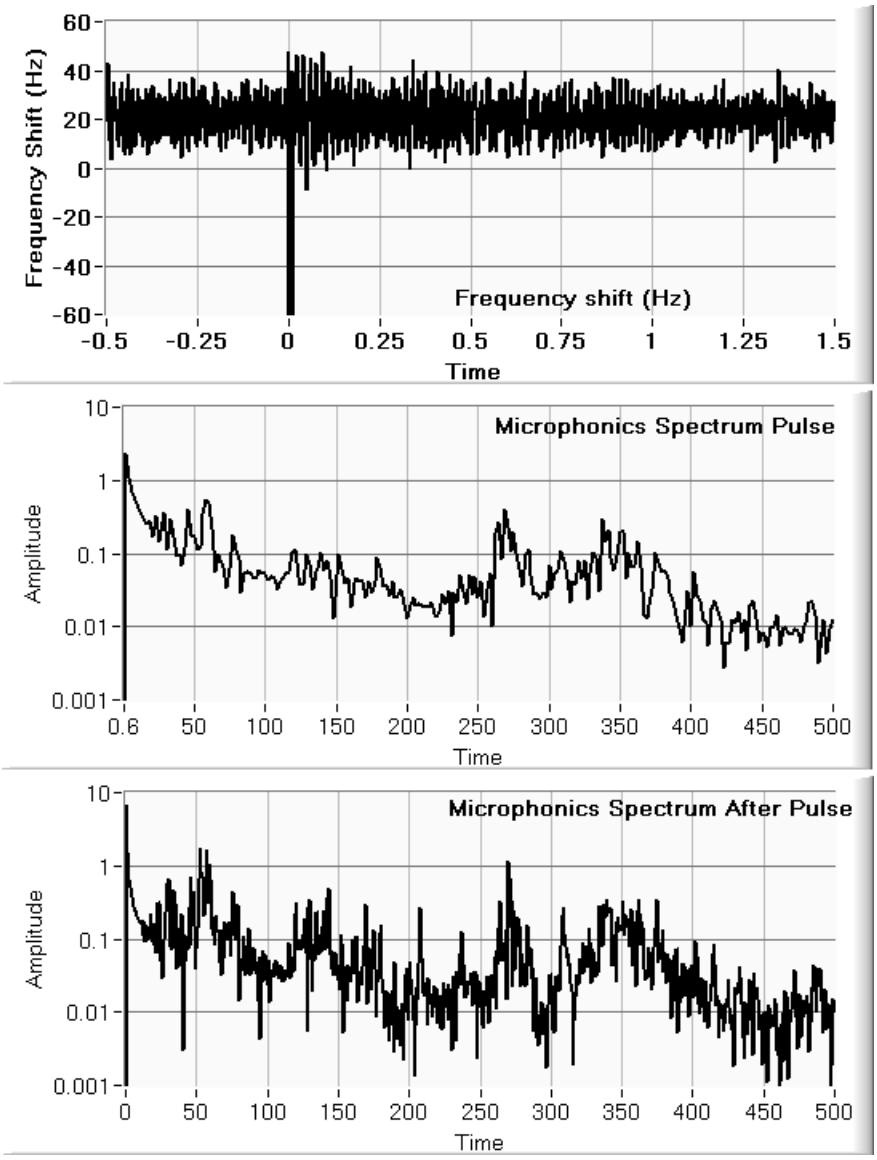

Figure 22. Time domain and frequency domain data for the entire record of the data shown in Figure 18.

Figure 23, 24 and 25 show the transients in cavity frequency after a test pulse, a waveguide vacuum arc and an electronic quench, respectively. Initially the RF was at a fixed frequency and controlled by the LLRF system. After the event, a VCO-PLL was used and the frequency tracked that of the cavity. The three significant pieces of information for each set of waveforms is show in table 1. The first are the fall times of the field probe power signal. One would expect that the VCO-VCO and the LLRF-VCO tests pulse decay times are the same at 1.1 ms. The fall time for the wavguide vacuum fault is longer because the plasma in the discharge does not present a matched impedance to the fundamental power coupler. The fall time for an electronic Quench was 80 μs. The rise time, which includes the VCO capture time, for all three types of events was approximately 3 ms.

The third significant item on the table is the peak-to-peak frequency shift. They range from 30 Hz for the background microphonics to 400 Hz for the electronic quench fault. Figure 26 depicts the results of processing the frequency shift data shown in figures 19, 24 and 25 using equation (8). It shows the calculated additional RF power required to compensate for the microphonic effects of the different types of events. Although not precisely equal the calculated results in Figure 26 is consistent with the data obtained in the closed loop test, Figures 11 and 12.

Event Type	**Gradient Decay Time**	**Gradient Fill Time**	**Peak to Peak Frequency Shift**
Background Microphonics	NA	NA	30 Hz
VCO-VCO test pulse	1 ms	3 ms	56 Hz
LLRF –VCO test pulse	1.1 ms	3 ms	45 Hz
Waveguide Vacuum Fault	1.9 ms	3 ms	75 Hz
Electronic Quench Fault	80 μs	3 ms	400 Hz

Table 1. Summary of microphonics effects.

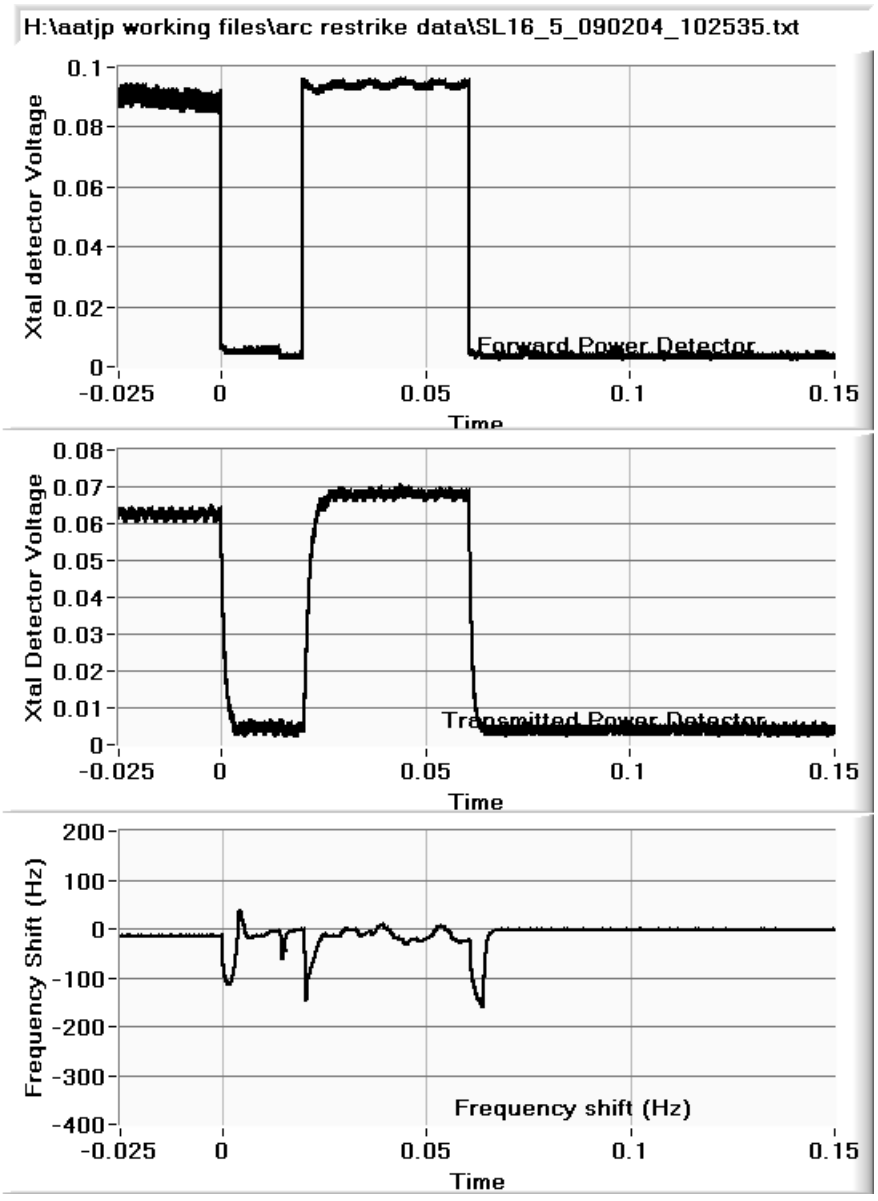

Figure 23. Response to an arc test pulse "trip". Peak to peak frequency shift of 45 Hz once gradient was established. The exponential time constant of the cavity field decay and fill were 1.1 ms and 3 ms respectively.

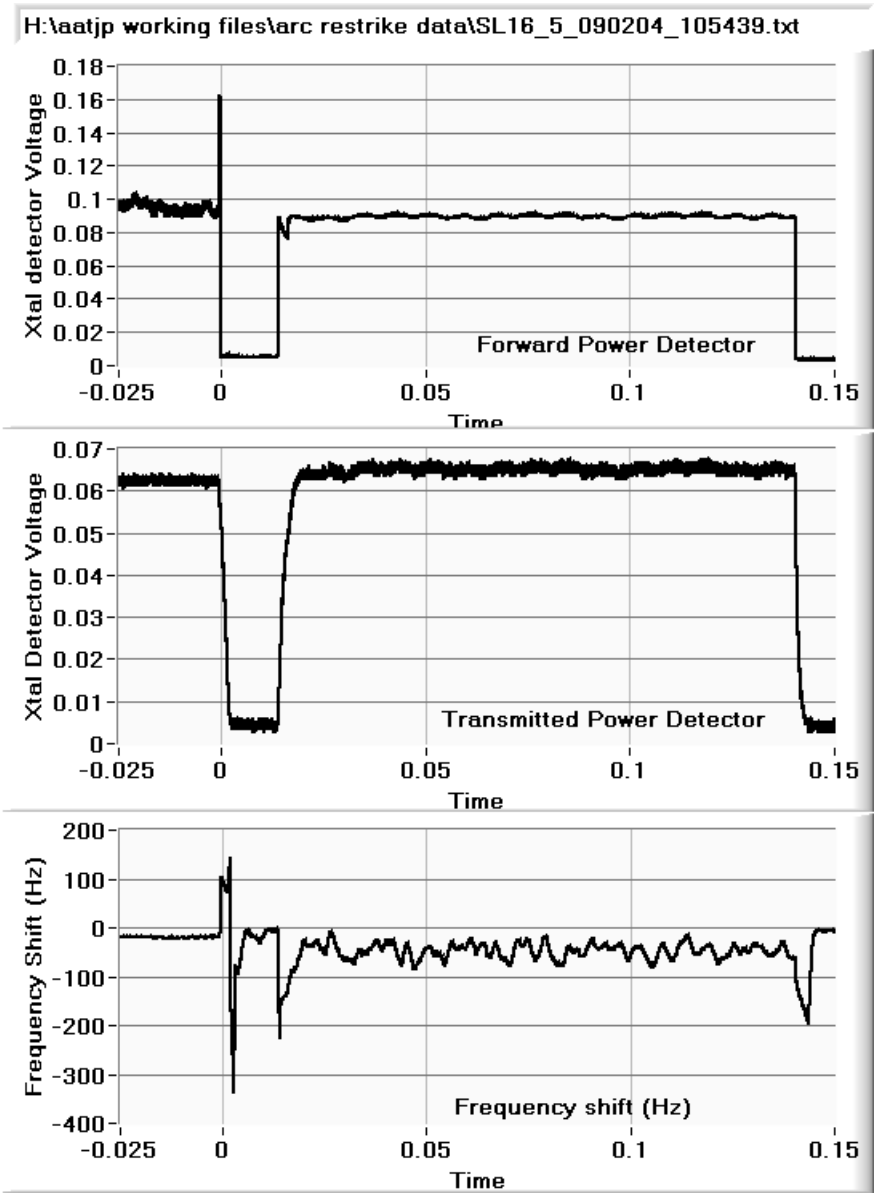

Figure 24. Response to waveguide vacuum arc. The peak to peak frequency shift was 75 Hz after gradient was established. The exponential time constant of the cavity field decay and fill were 1.9 ms and 3 ms respectively.

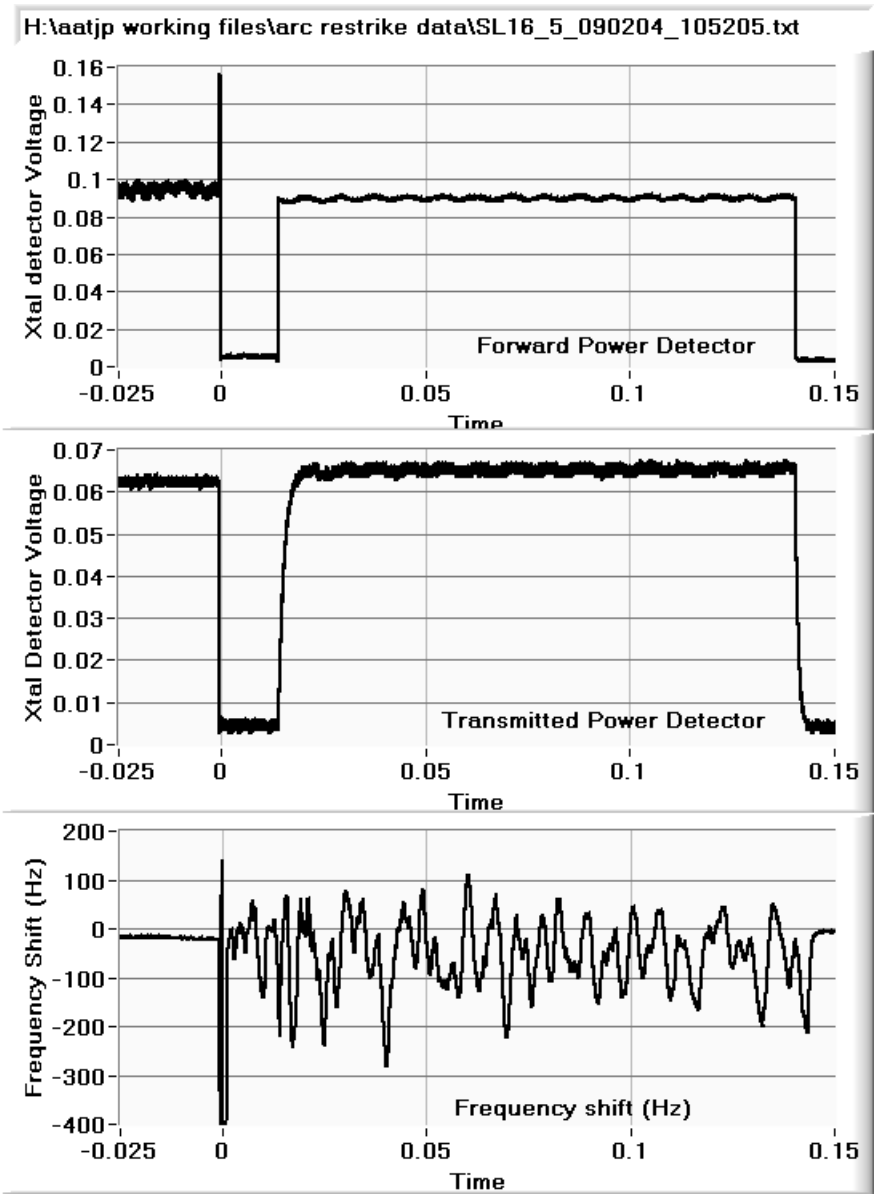

Figure 25. Response to an electronic quench. The peak to peak frequency shift was 400 Hz after gradient was established. The exponential time constant of the cavity field decay and fill were 80 μs and 3 ms respectively.

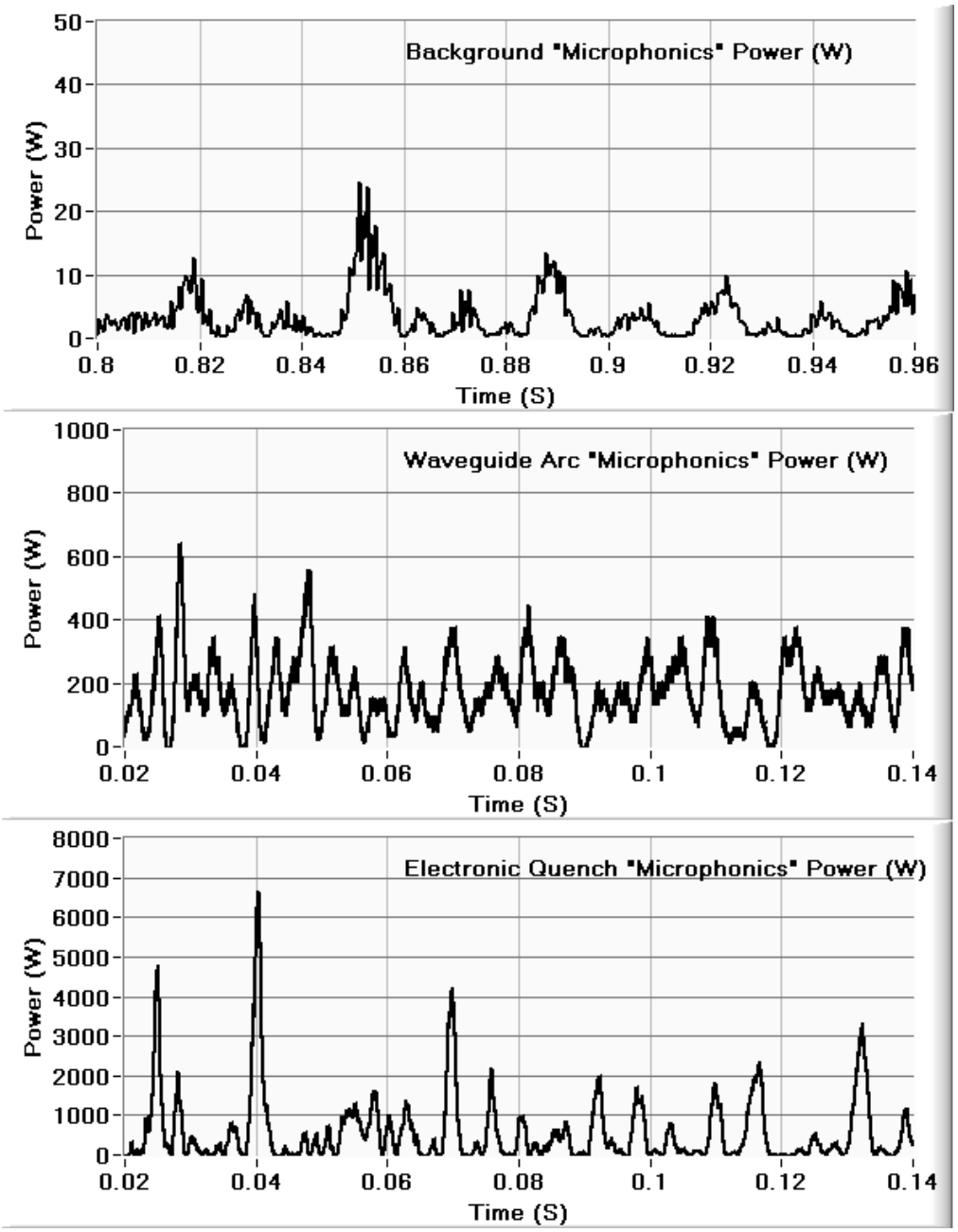

Figure 26. Calculated RF power required to compensate for the microphonics induced frequency shifts associated with the data shown in Figure 19, 24 and 25 respectively. The power levels were calculated using equation (8).

Summary of results.

The cavity gradient can be restored within about 20 ms of a waveguide vacuum fault. Thus, as previously thought, the vacuum characteristics of the waveguide are not a limiting factor when recovering the cavities for beam delivery. Microphonic effects have a dramatic impact on the recovery of a cavity after an arc fault. The hypothesis is that the rapid transient in the cavity gradient along with the pressure burst within the waveguide or cavity structures excite vibrational resonances in the cavity structure. The decay time of these vibrations is longer than 200 ms. Longer times were not tested due to a lack of cavity interlocks during the recovery test.

The baseline frequency shift due to microphonics on cavity SL16-5 was approximately 30 Hz peak to peak. The frequency shift due to microphonics after recovery from a "trip" due to an arc test pulse was 56 Hz peak to peak. The frequency shift due to microphonics after recovery from a waveguide vacuum fault was 75 Hz peak to peak. The frequency shift due to microphonics after recovery from an electronic quench was 400 Hz peak to peak. The nominal bandwidth of a CEBAF cavity is about 200 Hz. The calculated additional RF power required to maintain stable gradient was consistent with that obtained using a closed loop gradient control system.

It was not possible to restore stable gradient in the cavity after an electronic quench even after about 150 ms. Further, trying to restore full gradient after an electronic quench using closed loop gradient control system required large RF power levels which induced a secondary arc. Even when tests were run at gradient levels of 1.75 MV/m, as compared to the 6 MV/m steady state level, the cavity did not maintain gradient.

Operating the cavity using closed loop gradient control after a waveguide vacuum arc required twice the nominally budgeted forward power as compared to steady state operation. This additional power was required in order to compensate for frequency fluctuations due to microphonics effects. Power levels in excess of 10 times the nominal level were required in order to maintain closed loop control of the gradient after an electronic quench. These excess power requirements would cause klystron saturation driven instabilities in the RF system, if one were to try and establish beam prior to the vibrations decaying below levels budgeted for in LEM. Such instabilities lead to beam loss and beam loss accounting faults.

The bimodal effect in vacuum recovery time previously observed to be 100 ms and 250 ms [1] seems to be a related whether the fault was a waveguide vacuum fault or an electronic quench, with the longer decay times associated with waveguide vacuum arcs.

It may be possible to improve the RF recovery time for establishing stable gradient on a reasonable fraction of the arcing event to approximately 30 ms by making use of a fast reset algorithm. Those events are the waveguide vacuum arcs. Data recorded during this test as well as longer term parasitic testing in on cavity SL02-7 indicate that approximately half of the events recorded were waveguide vacuum arcs. A third data point is the results of the dedicated test of a cryounit in the cryomodule test facility done

in 1993. The test lasted several weeks. By the end of that test the majority of the arc events were initiated on the cavity side of the cold window.

Several factors, such as the waveguide vacuum signals and prompt detection of a cavity that does not properly achieve gradient, need to be addressed, if a fast automatic reset program is initiated. Of concern is that the existing optimized operation modes do not allow for sufficient microphonics headroom in order to maintain stable gradient in the presence of beam loading until the vibrations have decayed for at least 250 ms, possibly as long as a few seconds. Additionally, the fact that a cavity that was tested arced at a relatively low gradient is of concern. The microphonic effects due to Lorentz force detuning are proportional to the square of the gradient and thus will be approximately 3 times as bad at 10 MV/m.

Restoring the cavity gradient is only part of what has to be done in order to restore beam to the target. These other items are not included in the above stated recovery times. Additionally, there is only a limited amount of operational statistics for the ratio of waveguide vacuum arcs as compared to electronic quench driven arcs. Although not impossible, the results of this study are not encouraging with respect the ability for the CEBAF cavities to recover and deliver beam in times less than a few seconds.

References:

[1] E. F. Daly, D. Curry, J. Musson, G. Myneni, T. Powers, H. Wang, T. E. Whitlatch, I. E. Campisi, "Study of Arc-related RF Faults in the CEBAF Cryomodules", Proceedings of the 2004 European Particle Accelerator Conference, Aug. 2004, to be published.
[2] P. Kneisel, T. Powers, "Response of CEBAF's cold RF-window to operation in FE-regime of a cavity," CEBAF-TN-94-029.
[3] T. Powers, L. Phillips, C. Reece, P. Kneisel, V. Nguyen, "RF window arcing studies update: a comparison of results from cryomodule 17 and vertical cavity testing," CEBAF-TN-94-059.
[4] P. Kneisel, T. Powers, R. Allen, B. Lewis, "Cold RF-window arcing initiated by electron loading -- more evidence," CEBAF-TN-94-064.
[5] T. Powers, P. Kneisel, "Arcing phenomena on CEBAF RF-windows at cryogenic temperatures," CEBAF-TN-96-002.
[6] V. Nguyen-Tuong, N. Luo, L. Phillips, C. Reece, "Electronic activity at CEBAF cold RF window induced by cavity operation," CEBAF-TN-94-063.
[7] I. E. Campisi, M. Drury, P. Kneisel, J. Mammosser, T. Powers, J. Preble,
"Phoenix cryomodule post operations testing results or some results from the Phoenix retest," JLAB-TN97-01.
[8] L. Merminga, J. Delayen, "On the Optimization of Qext Under Heavy Beam Loading and In the Presence of Microphonics, CEBAF-TN96-022.
[9] J. Delayen, G. Davis, "Microphonics and Lorentz Transfer Function Measurements on the SNS Cryomodules, 11th Workshop on RF Superconductivity, Travenmunde, Lubeck (DE), 09/08/2003--09/12/2003 ; PBD: 1 Sep 2003